

# HI in the Outskirts of Nearby Galaxies

A. Bosma

**Abstract** The HI in disk galaxies frequently extends beyond the optical image, and can trace the dark matter there. I briefly highlight the history of high spatial resolution HI imaging, the contribution it made to the dark matter problem, and the current tension between several dynamical methods to break the disk-halo degeneracy. I then turn to the flaring problem, which could in principle probe the shape of the dark halo. Instead, however, a lot of attention is now devoted to understanding the role of gas accretion via galactic fountains. The current  $\Lambda$  cold dark matter theory has problems on galactic scales, such as the core-cusp problem, which can be addressed with HI observations of dwarf galaxies. For a similar range in rotation velocities, galaxies of type Sd have thin disks, while those of type Im are much thicker. After a few comments on modified Newtonian dynamics and on irregular galaxies, I close with statistics on the HI extent of galaxies.

## 1 Introduction

In this review, I will discuss the development of HI imaging in nearby galaxies, with emphasis on the galaxy outskirts, and take stock of the subject just before the start of the new surveys using novel instrumentation enabled by the developments in the framework of the Square Kilometer Array (SKA), which was originally partly inspired by HI imaging (Wilkinson 1991). I refer to other reviews on more specific subjects when appropriate. Issues related to star formation are dealt with by Elmegreen and Hunter (this volume), and Koda and Watson (this volume).

In the late 1950s, it became clear that there was more to a galaxy than just its optical image. This was principally due to the prediction of the 21 cm HI hyperfine structure line by Van de Hulst in 1944, and its detection in the Milky Way (Ewen

---

A. Bosma

Aix Marseille Univ, CNRS, LAM, Laboratoire d'Astrophysique de Marseille, Marseille, France,  
e-mail: bosma@lam.fr

and Purcell 1951; Muller and Oort 1951). A first rotation curve of the Milky Way was determined by Kwee et al. (1954). The first observations of M31 were done using the Dwingeloo 25 m telescope (van de Hulst et al. 1957), and a mass model for this galaxy considered by Schmidt (1957). A possible increase in the mass-to-light ( $M/L$ ) ratio in the outermost parts of M31 prompted the photoelectric study of its light distribution by de Vaucouleurs (1958), who confirmed that the local  $M/L$  ratio at the last point measured by Van de Hulst et al. exceeds the expectation from a model with constant  $M/L$  ratio throughout this galaxy's disk, in contrast with an earlier model by Schwarzschild (1954). The outer HI layer of the Milky Way was found to be warped (Burke 1957; Kerr 1957), and flaring (Gum et al. 1960). Dark matter in the Local Group was inferred by Kahn and Woltjer (1959), who attributed the high mass of the Local group to intergalactic gas, and explained the warp as due to our Milky Way moving through it.

## 2 HI in Galaxies and the Dark Matter Problem: Early Work

Early HI work on external galaxies was done with single-dish telescopes, often prone to side lobe effects (cf. discussion after Salpeter 1978). Progress was slow, and hampered by low spatial resolution—a small ratio of HI radius to beam size (Bosma 1978, his Chapter 3.4)—of the observations. With the Dwingeloo telescope, work on M31 was followed by major axis measurements of M33 and M101 (Volders 1959). The Parkes telescope was used to image the LMC (McGee and Milton 1966), the SMC (Hindman 1967), NGC 300 (Shobbrook and Robinson 1967), and M83 (Lewis 1968). In the northern hemisphere, data were reported for several galaxies by Roberts (1966, for M31), Roberts (1972) and Davies (1974). In an Appendix, Freeman (1970) discusses rotation data for the LMC, SMC, NGC 300 and M33, and, for the latter two galaxies, found that the turnover velocity indicated by the low-resolution HI data is larger than the one indicated by fitting an exponential disk to the optical surface photometry, suggesting the presence of matter in the outer parts with a different distribution than that in the inner parts.

The quest for higher spatial resolution was first achieved routinely with the Caltech interferometer, (e.g., for M101, Rogstad and Shostak 1971; Rogstad 1971), and results for five Scd galaxies were summarized in Rogstad and Shostak (1972), who found high  $M/L$  material in the outer parts of these galaxies. Work began on M31 with the Cambridge half-mile telescope with a first report (Emerson and Baldwin 1973) showing “normal”  $M/L$  values. Their data were in disagreement with data by Roberts on the same galaxy, as debated in a meeting in Besançon (Roberts 1975; Baldwin 1975). This problem was settled by new data reported by Newton and Emerson (1977), who by and large confirmed the data of Roberts and Whitehurst (1975). Meanwhile, HI work with the Westerbork Synthesis Radio Telescope (WSRT) had started, with as first target M81. The resulting rotation data, extending beyond the optical image, were discussed in Roberts and Rots (1973), with curves for M31 (300 ft data), M81 (WSRT and 300 ft data), M101 (from Rogstad's Caltech

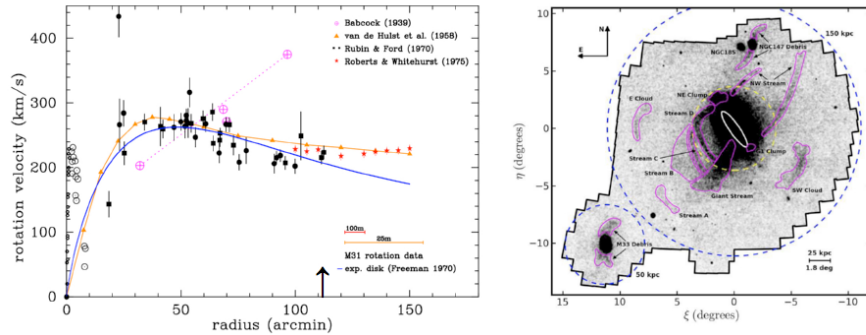


**Fig. 1** *Left panel:* rotation curves of M31, as determined by Babcock (1939, purple points), van de Hulst et al. (1957, orange points), Rubin and Ford (1970, black points), and Roberts and Whitehurst (1975, red points). The blue line indicates the expected maximum disk rotation curve based on an exponential disk with the scale length given in Freeman (1970) based on the study of de Vaucouleurs (1958). The arrow indicates the optical radius. *Right panel:* modern picture of the outskirts of M31, as determined from the PAndAS survey (reproduced with permission from Ferguson and Mackey 2016), where the outline of the optical image is in white. Note the change in scale

data) and the Milky Way. These data, in particular for M31, also suggested that there could be more than meets the eye in the outer parts of galaxies, i.e., material with high  $M/L$  ratio (cf. Fig. 1, left panel).

A second line of argument for material with high  $M/L$  ratio in the outer parts of galaxies came from theory. Early numerical experiments, e.g., by Hohl (1971), showed that simulating a galaxy disk with  $N$ -body particles and letting it evolve generated the formation of a bar-like structure with relatively high velocity dispersion. Since strong bars are present only in about 30% of the disk galaxies, Ostriker and Peebles (1973) proposed to stabilize the disk by immersing it in a halo of “dark matter”, in such a way that the gravitational forces of the halo material acting on the disk could prohibit the bar to form. This requires that out to the radius of the “optical” disk, the mass of the halo is 1 – 2.5 times the disk mass. Once hypothesized, it followed that the masses of galaxies exterior to this radius could be extremely large. This was subsequently investigated by Einasto et al. (1974), as well as Ostriker et al. (1974). While the former considered five galaxies, amongst which IC 342, and data on binary galaxies, the latter put forward at least half a dozen probes (the rotation curve data discussed above, the Local Group timing argument already considered in Kahn and Woltjer 1959, binary galaxy samples, etc.). Both papers concluded that there must be additional, dark, matter beyond the optical radius of a galaxy, since the mass increases almost linearly with radius, and the light converges asymptotically.

Athanassoula (2002, 2003), using much-improved  $N$ -body simulations with live haloes (i.e., haloes responding to gravitational forces), confirmed the above results for the initial phases of the evolution. She found, however, that at later times, when the bar evolves and increases in strength, the halo material at resonance with the bar will actually help the bar grow and become stronger. Hence the theoretical picture in Ostriker and Peebles (1973) is now superseded. Likewise, Athanassoula (2008)

showed that the Efstathiou-Lake-Negroponte global stability criterion (Efstathiou et al. 1982), popular in semi-analytic galaxy formation models of galaxies, is not really valid.

Although some cosmologists developed the theory of galaxy formation, and came up with a two-stage model (e.g., White and Rees 1978), the debate about the validity of the data, and even the notion of dark matter itself, continued for several years, witness papers disputing the idea (e.g., Burbidge 1975; Materne and Tammann 1976). New data on this topic came from efforts improving the statistics of binary galaxies and clusters of galaxies, but the most convincing evidence came from fresh data on the rotation curves of spiral galaxies, discussed in Sect. 4.

### 3 Warps

One observational problem hindering the acceptance of the existence of the dark matter indicated by the HI data concerned the presence of large-scale non-circular motions in the outer parts, as frequently emphasized by sceptical observers (e.g., Baldwin 1974, 1975). Einasto et al. (1974) simply rejected this hypothesis—without stating a reason—even though the one galaxy they show data for, IC 342, was found to be clearly warped (Newton 1980).

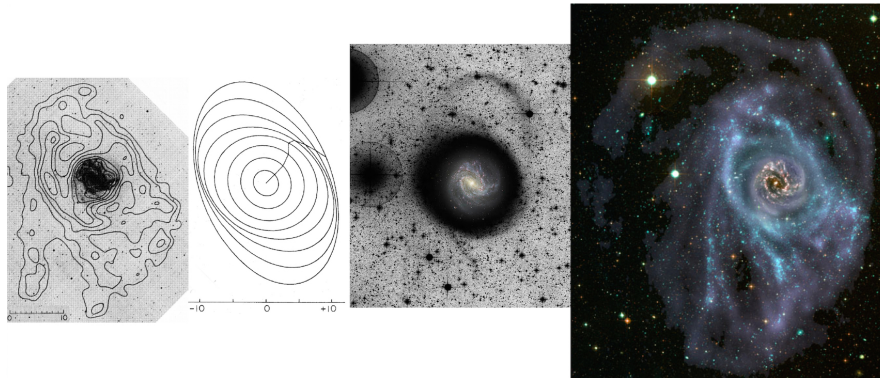


**Fig. 2** *Left* two panels: HI distribution and tilted ring model of M83 (reproduced with permission from Rogstad et al. 1974); next to it a deep optical image obtained by Malin and Hadley (1997) with a shallower colour image superimposed (credit: D. Malin). The *rightmost* image was constructed from *GALEX* UV data, optical images, and the HI distribution obtained in the Local Volume HI Survey conducted with CSIRO’s Australia Telescope Compact Array (ATCA; credit: B. Koribalski and A. R. López-Sánchez). All images are on the same scale

Rogstad et al. (1974) came up with a novel approach to model the velocity field of M83, using new data obtained with the two-element Owens Valley interferometer. They introduced the notion of what later was called the “tilted ring model”, by modelling a galaxy with a set of concentric annuli each having a different spatial

orientation. Although they were forced to use a model rotation curve on account of M83's low inclination, later on rotation curves were derived by determining the rotation velocity for each annulus separately (Bosma 1978, 1981a). It is of interest to display the results of Rogstad et al. (1974) side by side with more modern results, as has been arranged in Fig. 2. Since the outer contour in the 1974 HI image is  $1.37 \times 10^{20} \text{ cm}^{-2}$ , the presence of extended HI disks in M83-like systems is detectable with the upcoming large HI surveys, even for those with shorter integration times such as planned for the APERTIF-SNS and WALLABY surveys.



**Fig. 3** *Left*: two HI channel maps at either side of the systemic velocity of NGC 5907, superimposed on an optical image of the galaxy, indicate clearly the presence of a warp in the HI distribution (reproduced with permission from Sancisi 1976). *Right*: at the same scale, a deep optical image showing the presence of a diffuse tidal stellar stream around this galaxy (reproduced with permission from Martínez-Delgado et al. 2008)

The first study of HI warps in spiral galaxies seen edge-on was done by Sancisi (1976), whose clearest case was NGC 5907. This galaxy has subsequently been studied extensively in the optical regime, in order to find the presence of extraplanar light. A “faint glow” was found by Sackett et al. (1994a), whose report made the cover of *Nature*, but later work by Zheng et al. (1999) indicated the presence of an arc. A deeper picture was published by Martínez-Delgado et al. (2008), and is reproduced in Fig. 3. Further modelling of the warp has been done in Allaert et al. (2015). The surmise in Sancisi (1976) that warps are occurring in galaxies seemingly free of signs of interactions thus turns out to be not justified, but the stellar mass involved in the stream appears minor compared to that in the main galaxy. As is the case for M83, the streamer indicates a past interaction or merging event, a process which could have caused the warp as well.

Rogstad et al. (1976, 1979) found warps in M33 and NGC 300, and I found several more during my thesis work, as discussed below. Briggs (1990) outlined a set of “rules of behaviour” for warps by studying HI images of a number of warped galaxies studied by the end of the 1980s. They start in the region beyond the optical radius ( $r_{\text{opt}}$ ), and become prominent at the Holmberg radius ( $r_{\text{Ho}}$ ), while the line-of-nodes turns in such a manner that the direction in which it is turning is leading with

respect to the spiral arms. This behaviour is due to differential precession, as already noted in Kahn and Woltjer (1959) and was privately discussed in 1976 between Rogstad and Bosma for five cases then known. Newton (1980) shows clearly that the data of IC 342 do not support this picture, but his work was not considered by Briggs (1990). Note that for the giant low surface brightness disk galaxy Malin 1, the HI velocity field observed by Lelli et al. (2010) shows clearly that this galaxy also violates Briggs’s rule no. 3, and that the faint giant low surface brightness disk imaged recently by Galaz et al. (2015) is in the warped part of the galaxy.

#### 4 Further Data on HI in Galaxies and the Dark Matter Problem

In my thesis work (Bosma 1978, 1981a,b) I collected extensive HI data on a number of galaxies using the WSRT and its 80-channel receiver. I produced warp models using tilted ring models, and derived mass models from rotation curves ignoring possible vertical motions associated with the warps. For the photometry, new observations were obtained (cf. van der Kruit 1979), and the resulting plot of the local  $M/L$  ratios was reported in Bosma (1978) and Bosma and van der Kruit (1979). I augmented the sample with literature data so as to arrive at a comprehensive figure of 25 rotation curves split over six panels of different morphological types. This Figure was reproduced in an influential review article by Faber and Gallagher (1979), and gained widespread attention. The local  $M/L$  ratios in the outer parts of galaxies were found to be very large in quite a number of cases, establishing the presence of dark matter.

At present, such data are considered as primary evidence for the presence of dark matter in spiral galaxies. Contemporary data by Rubin et al. (1978), followed by a systematic study of galaxies of type Sc (Rubin et al. 1980), Sb (Rubin et al. 1982) and Sa (Rubin et al. 1985) show also flat and rising rotation curves, but it has been convincingly shown, first by Kalnajs (1983) and later by Kent (1986, 1987, 1988), as well as by Athanassoula et al. (1987), that for most of the galaxies in Rubin’s survey the data do not go out far enough in radius to unambiguously demonstrate the need for dark matter (see also Bertone and Hooper 2016).

For this review, I will concentrate on the most extended HI disks found in Bosma (1978, 1981a,b), and show as example the galaxy NGC 2841 (Fig. 4). The HI extends out to  $\sim 2.5$  times the Holmberg radius, i.e.,  $\sim 3.5 \times r_{\text{opt}}$ . The tilted ring model describing the warp leaves out the northernmost feature, an asymmetry further emphasized in Baldwin et al. (1980), although of much smaller amplitude than that in the HI distribution in M101. A similar extended HI disk was found for NGC 5055 (Fig. 5), which became later a prototype of a Type I extended UV disk (Thilker et al. 2007), and for which Martínez-Delgado et al. (2010) found extensive streamers, some of which are not associated with the HI gas or the young stars. In Bosma (1978, 1981b) I summarize data on the extent of the HI disks in my sample, and found a wide variety of values of the ratio  $r_{\text{HI}}/r_{\text{opt}}$ , where  $r_{\text{HI}}$  is defined as the

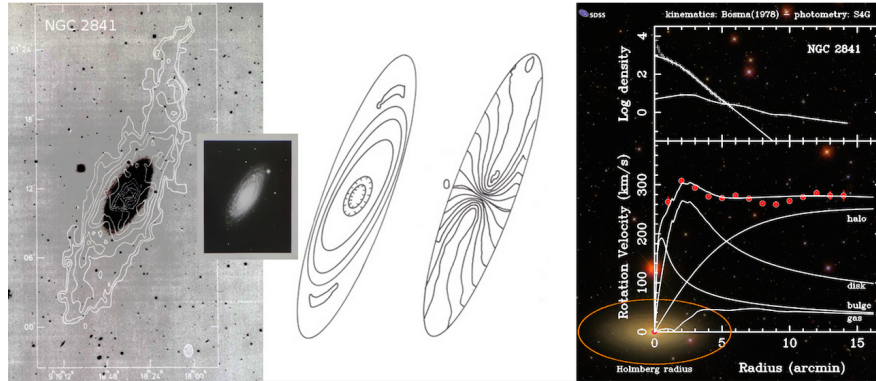


**Fig. 4** At left, the HI distribution in the galaxy NGC 2841 observed by Bosma (1978), overlaid on a deep IIIaJ image provided by H.C. Arp; the inset shows the Hubble Atlas image (Sandage 1961). The middle panels show the warp model. At right a mass model of the galaxy adjusted to the HI rotation data in Bosma (1978), calculated as described in Athanassoula et al. (1987), using surface photometry data from the *Spitzer* Survey of Stellar Structure in Galaxies (S<sup>4</sup>G; Muñoz-Mateos et al. 2015), and overlaid on scale on a Sloan Digital Sky Survey (SDSS) colour image. The orange ellipse around the galaxy outlines the Holmberg (1958) dimensions. Montage as in Roberts (1988), suggested in this form by Bernard Jones (private communication)

isophote where the HI column density is  $1.82 \times 10^{20} \text{ cm}^{-2}$ , with a mean of  $2.2 \pm 1.1$ .

## 5 The Disk-Halo Degeneracy in the Dark Matter Problem

Van Albada and Sancisi (1986) pointed out that mass modelling based on the assumption that the  $M/L$  ratio is constant as function of radius in the disk contains a degeneracy: it is a priori not clear whether a maximum disk, i.e., a disk so massive that its rotation curve fits the inner parts of the observed one without overshooting it, is the correct answer. Already it is not entirely justified to assume that the  $M/L$  ratio is constant throughout the disk, even though this is customary, since if there is a colour gradient in bright spirals, it is usually in the sense that the outer parts are bluer. Yet another problem is that the assumption of maximum disk generally leads to haloes which are cored, and thus do not follow a Navarro-Frenk-White (NFW) model (e.g., Navarro 1998).

This disk-halo degeneracy is a serious problem which is even now under debate. Relating a value of the  $M/L$  ratio to a disk colour, and working out whether “reasonable” stellar populations can then be assumed, does not appear entirely satisfactory, due to possible variations in the initial mass function (IMF). Various groups have thus tried to marshal dynamical arguments to break the degeneracy, but the answers are mixed. Mechanisms of spiral structure generation, in particular the swing amplifier mechanism (Toomre 1981), depend on the ratio of disk mass to halo mass.

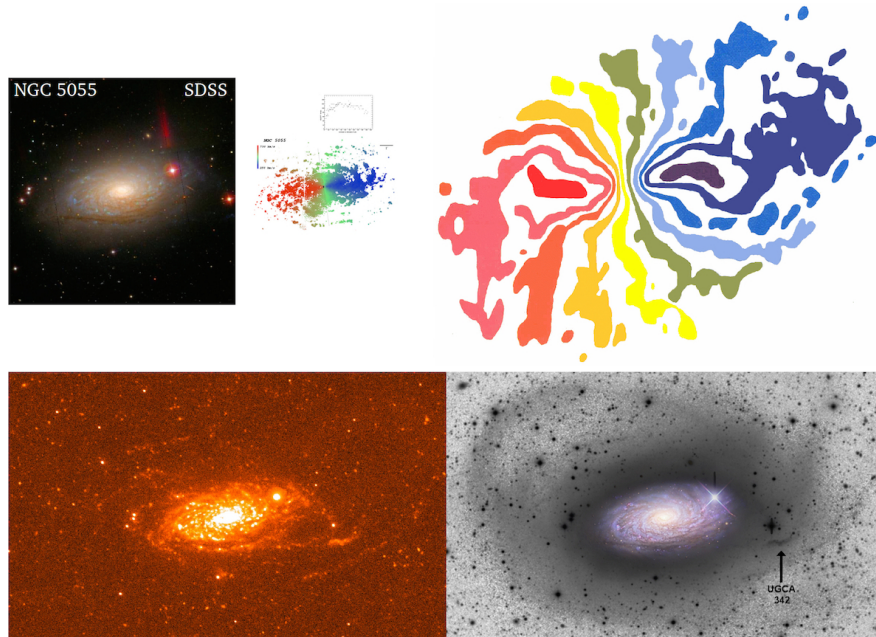


**Fig. 5** *Top left*, a SDSS colour image of NGC 5055, with next to it a representation of the  $H\alpha$  velocity field from the GHASP survey (reproduced with permission from Blais-Ouellette et al. 2004), and just above it the  $H\alpha$  rotation curve of Burbidge et al. (1960). The *top right* panel shows the velocity field of NGC 5055 shown on the front cover of Bosma (1978). The colour lookup table used there is such that the boundaries of each coloured patch correspond to equispaced isovelocity contours. *Bottom left* is the *GALEX* near-UV image (data taken from the NASA/IPAC Extragalactic Database, NED) and *bottom right* a deep optical image from Martínez-Delgado et al. (2010) (credit: D. Martínez-Delgado and T. Chonis). All images are on the same scale. The star-forming patch west of the centre of NGC 5055, UGCA 342, can already be seen on the deep IIIaJ image (van der Kruit 1979) also shown as Fig. 4.3.1b in Bosma (1978)

Athanassoula et al. (1987) used this in detail to set a range of allowed values of the disk/halo mass ratio, by remarking that most spirals are dominated by an  $m = 2$  component, and thus requiring that an  $m = 2$  spiral be allowed to amplify, while at the upper end suppressing an  $m = 1$  component. This is further discussed in Bosma (1999) and illustrated in Fig. 6 (top right panel).

Fuller dynamical modelling has been done for a number of galaxies. Kranz et al. (2003) calculated spiral structure models based on potentials derived from  $K'$ -band photometry and compared the gas flow in these with the observed velocity fields for a sample of five galaxies. Similarly, for bars, the gas flow can be calculated in a potential derived from imaging in the near- or mid-infrared. Seeking to fit the amplitude of the jump in radial velocity across a dust lane, which outlines the location of a shock in the flow, will constrain the  $M/L$  ratio of the disk (Lindblad et al. 1996; Weiner et al. 2001; Weiner 2004; Zánmar Sánchez et al. 2008). For the face-on barred spiral NGC 1291, Fragkoudi et al. (2016) calculated a range of models try-

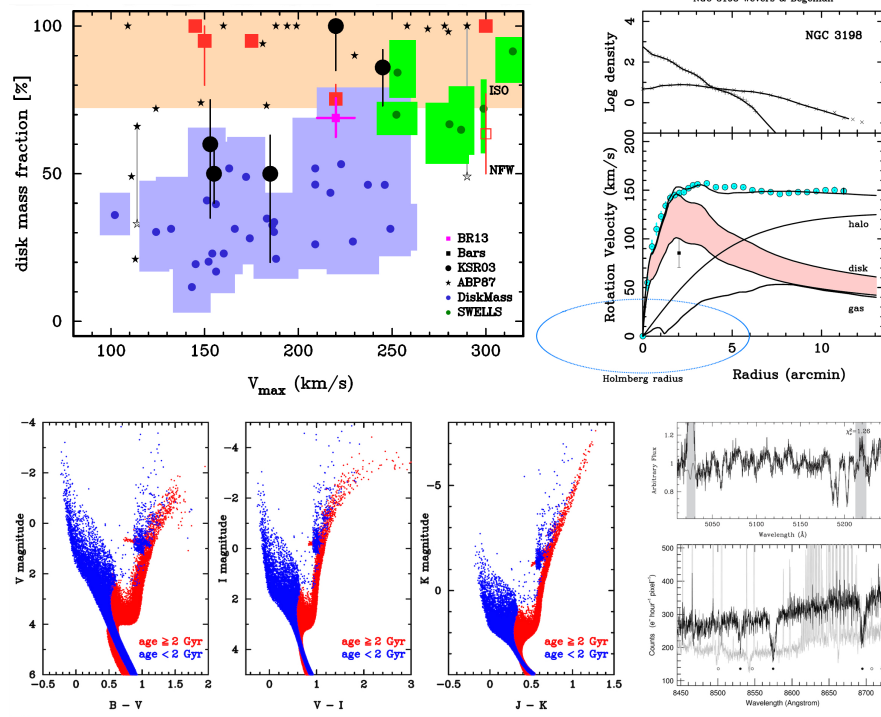


**Fig. 6** *Top left*: disk mass fraction as function of the maximum velocity of the rotation curve, determined with several methods. “BR13” (Bovy and Rix 2013) indicates the value for our Galaxy. “Bars” concern the determination using gas flow models in barred spirals (see text). “KSR03” concern five galaxies studied by Kranz et al. (2003). Black filled stars concern the results from Athanassoula et al. (1987) for their “maximum disk with no  $m = 1$ ” models, except for two vertical lines at  $V_{\max} = 114.0$  and  $280.0$  km/s which indicate also the “no  $m = 2$ ” models. For the DiskMass project, the results are taken as in Courteau and Dutton (2015), but the error bars are replaced by the area spanned by them. A similar representation has been done for the SWELLS survey (Barnabè et al. 2012; Dutton et al. 2013). *Top right*: mass models for NGC 3198 according to the method described in Athanassoula et al. (1987), and shown in detail in Bosma (1999); *Bottom left*: colour-magnitude diagrams calculated with IAC-STAR (Aparicio and Gallart 2004) in a manner similar to that used in Aniyán et al. (2016). *Bottom right*: spectra obtained by Westfall et al. (2011) in the MgI region, and by Bershadsky et al. (2005) in the CaII region (reproduced by permission)

ing to fit the shape of the dust lane. Most of the barred spiral models require close to maximum disk, while for the spiral models a range of values depending on the maximum rotational velocity has been found, as shown in Fig. 6 (top left panel).

The study of the lensing galaxy associated with the quad-lens Q2237+0305 done by Trott et al. (2010) shows that at least the central part of that galaxy needs a maximum  $M/L$  value. Note that that galaxy is barred, and its bulge thus presumably of the boxy/peanut type. Barnabè et al. (2012) and Dutton et al. (2013) also find maximum bulges in the SWELLS survey. Dutton et al. (2013) suggest that the IMF in bulges is more like the Salpeter one, and in disks is closer to the Chabrier one.

The major method favouring non-maximum disks is based on the analysis of stellar velocity dispersions. This is not straightforward, since one has to assume either a disk thickness when the galaxy is face-on, or a ratio of radial to vertical velocity dispersion when the galaxy is edge-on. The results of Bottema (1993, 1997), Kregel et al. (2005) and the more recent DiskMass project (Bershady et al. 2011; Martinsson et al. 2013, and references therein) all point to sub-maximum disks. Yet doubts have been expressed, as in Bosma (1999), from which we quote

... as argued by Kormendy (private communication, see also Fuchs's contribution—Fuchs 1999), the influence of younger stellar populations could result in lower measured velocity dispersions.

Aniyan et al. (2016) recently quantified this concern, and I show in Fig. 6 (lower left panel) a variation on their principal result. As argued in Aniyan et al., the stellar populations in the blue-visible region, where the MgI velocity dispersion is measured, are heavily contaminated by the presence of young stars, which might have lower velocity dispersions than the old stars. On the other hand, in the infrared (e.g., *K*-band), the light of the red giant branch stars dominate. Hence there is a mismatch between the stellar populations used to measure the velocity dispersion and those used to estimate the disk scale height, with as a result that the  $M/L$  ratio of the disk is underestimated. Calculations by Aniyan et al. (2016) show that this can roughly explain the difference between the results of the DiskMass project (sub-maximum disks), and those from several other dynamical estimators (maximum disks).

Although the authors of the DiskMass project were aware of a stellar population effect, witness the extensive discussions of this in, e.g., Bershady et al. (2005, 2010a,b) and Westfall et al. (2011), they argue clearly for the use of the MgI region as the preferred region for doing velocity dispersion work, since the CaII region has 1) larger intrinsic line widths, 2) a higher background, and 3) more scattered light (cf. Bershady et al. 2005, and the spectra shown in Fig. 6, lower right panel). Most galaxies they discuss have been observed only in the MgI region, and, in the few cases where data at both wavelength regions were available, no difference was noticed.

It should be possible, however, to investigate a possible systematic effect of stellar population differences on the velocity dispersions further, since even in the *i*-band the older stellar populations are substantially more prominent than in the *g*-band (see Fig. 6, lower row, second panel from left). There are now several spectrographs being built which will have a setup allowing the simultaneous measurement of the velocity dispersions of the same galaxy in both the MgI region and the CaII region. In particular, the WEAVE spectrograph (Dalton 2016) has high spectral resolution, and can thus suitably be used to test whether CaII-derived velocity dispersion measurements are systematically larger than MgI-derived ones in face-on spiral galaxies.

## 6 Flaring of the Outer HI Layer: Probing the Shape of the Dark Matter Halo

As mentioned in Sect. 1, a flaring HI disk was found in the Milky Way (Gum et al. 1960). An early study of the flaring HI disk in the edge-on galaxy NGC 891 was made by van der Kruit (1981), who found that the HI thickness as function of radius observed by Sancisi and Allen (1979) could best be modelled by assuming that the disk potential was furnished mainly by the old stellar disk. For the face-on galaxies NGC 3938, NGC 628 and NGC 1058 a constant gas velocity dispersion as function of radius was found, of order 10 km/s (van der Kruit and Shostak 1982; Shostak and van der Kruit 1984; van der Kruit and Shostak 1984). It was thus thought that flaring HI disks could be used to probe the shape of the dark halo.

### 6.1 Early Work on Case Studies

With the advent of the high-sensitivity, high-resolution capabilities of the Very Large Array (VLA), NGC 4565 and NGC 891 were re-observed by Rupen (1991). These observations indicated clearly the warps in these systems, as well as asymmetries in the HI distribution. A further effort was made by Olling (1996a,b) for the small galaxy NGC 4244, who found that the best fit was a very flattened halo, with an axial ratio  $c/a$  of  $\sim 0.2$ . Becquaert and Combes (1997) found a similar result for NGC 891, but if the vertical velocity dispersion was smaller than the radial one, a value of  $\sim 0.4$ - $0.5$  could be found. Applying the same technique to observations of our Galaxy, Olling and Merrifield (2000) found a relatively round halo ( $c/a \sim 0.8$ ), but needed to adopt rather low values for some Galactic constants. Using a completely different method (lensing and optical spectroscopy) for the massive galaxy SDSS J2141-0001, Barnabè et al. (2012) recently found an oblate dark halo, with  $c/a = 0.75 \pm_{0.16}^{0.27}$ .

Also in the 1980s-90s, efforts were made to use another probe of the shape of the dark matter halo, i.e., polar ring galaxies. Here, there was a remarkable shift of the “most likely” halo shape: the early studies of the polar ring galaxy A0136-0801 by Schweizer et al. (1983), and a few others (Whitmore et al. 1987) indicated a nearly round halo, while a later study of Sackett et al. (1994b) showed the halo around NGC 4650A as flat as E6. However, Arnaboldi et al. (1997) showed that the polar ring in that galaxy is very massive, and has spiral structure. Khoperskov et al. (2014) worked on a larger sample, and showed that a variety of halo shapes describe the data.

The expected HI disk flaring was calculated for NGC 3198 and DDO 154 by Bosma (1994), and the result for NGC 3198, based on the maximum disk model in Fig. 6 (top right panel), is shown in Fig. 7. This calculation assumes equilibrium, and shows that the flaring depends on the velocity dispersion of the HI disk, as well as the axial ratio of the dark halo. For a dwarf galaxy, assumed also to be flat, the

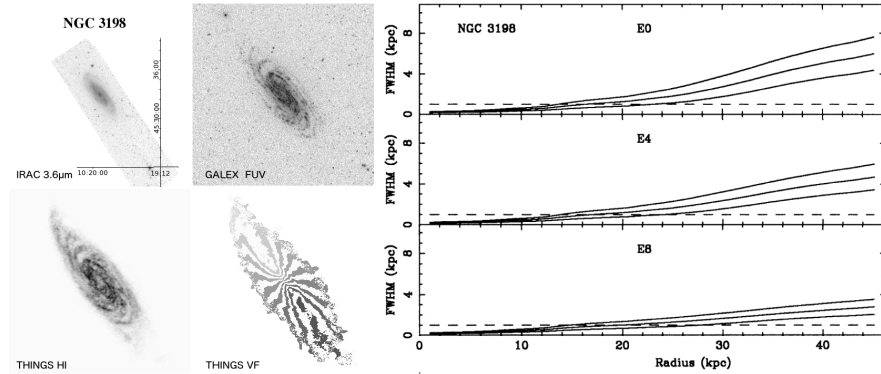


**Fig. 7** *Spitzer* 3.6  $\mu\text{m}$ , *GALEX* far-UV, and HI data from the THINGS survey for NGC 3198 (data taken from NED). At *right* is the flaring calculation from Bosma 1994, using the mass model in the top right panel of Fig. 6. The three curves are for constant velocity dispersions of 6, 8 and 10 km/s, and the halo flattening is expressed as for elliptical galaxies

flaring starts well inside the optical radius, since the dark matter dominates also in the inner parts of the disk. Thus the study of small, thin edge-on galaxies seems ideal for this problem.

## 6.2 Recent Results for Small, Flat Galaxies

“Super thin” galaxies were studied initially by Goad and Roberts (1981), and later investigated by, e.g., Uson and Matthews (2003), Matthews and Wood (2003), Matthews and Uson (2008) and in thesis work by O’Brien et al. (2010a,b,c,d) and Peters et al. (2013, 2016a,b,c,d). A lot of work hides behind these results, since HI disks are frequently warped, and candidate galaxies have to be observed first before judging whether they are suitable for further study for the flaring problem. Even if the obviously warped galaxies are excluded from further study in this respect, subtle variations can influence the result. Matthews and Wood (2003) thus considered for their best case, UGC 7321, several models: a smooth distribution, a warped one, a flaring one, and a model with an HI halo, which either corotates or lags, and combinations of these. None of them give a very satisfactory fit if attention is paid to detail. O’Brien et al. (2010d) found  $c/a = 1.0 \pm 0.1$  for their best case, again UGC 7321. Peters et al. (2013) extended the database of O’Brien et al, but Peters et al. (2016d) found in the end only good flaring models for two galaxies, ESO 274-G001 and UGC 7321. For ESO 274-G001, they found an oblate halo with shape  $c/a = 0.7 \pm 0.1$ , while for UGC 7321 they found a prolate halo, with  $c/a = 1.9 \pm_{0.3}^{0.1}$  in case the HI is treated as optically thin, and  $2.0 \pm 0.1$  in case the optical thickness of the HI is taken into account. They point out that O’Brien et al. (2010d) did not consider prolate halo shapes, hence the difference.

Most of these late-type Sd galaxies have small maximum rotation velocities, and low star formation activity. Systematic studies by Karachentsev et al. (1999) have resulted in an extensive catalogue of these flat galaxies. Such data can be explored further in the era of large galaxy surveys.

Peters et al. (2016a) emphasize that it cannot be assumed that the HI in galaxies is optically thin, and constructed a modelling procedure. Braun (1997) already emphasized this point twenty years ago in a study of seven nearby spiral galaxies at high spatial and spectral resolution with the VLA, and argued that there is significant opacity in the high surface brightness HI gas. Braun et al. (2009) show this in their M31 data with specific examples, and estimate that the total HI gas mass in that galaxy is about 30% higher than the value inferred using the assumption of optically thin gas.

### 6.3 Large Galaxies with a High Star Formation Rate: Accretion

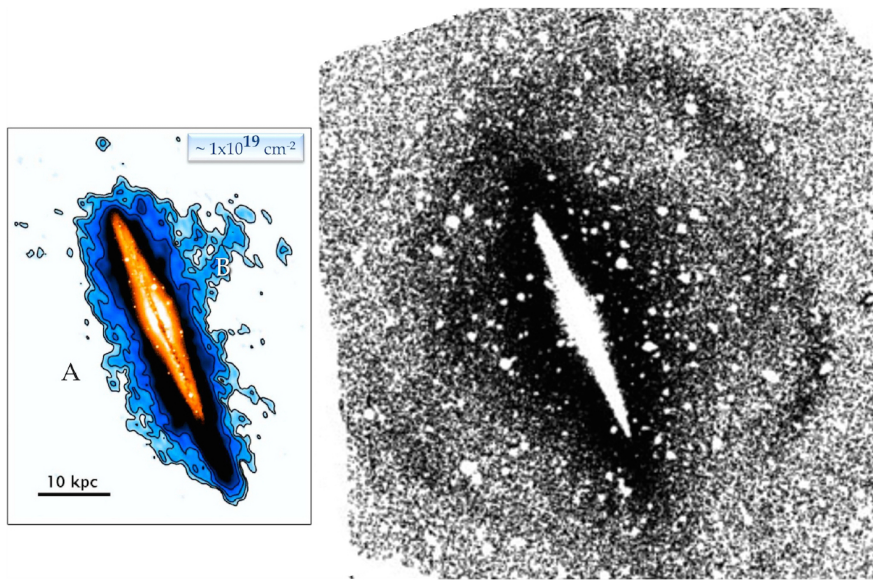


**Fig. 8** At *left* the HI image of NGC 891 (reproduced with permission from Oosterloo et al. 2007), with an outer contour column density of  $1.0 \times 10^{19} \text{ cm}^{-2}$ , and at *right*, on the same scale, the image of the RGB stars (reproduced with permission from Mouhcine et al. 2010)

Deep imaging (for that time) of M101 (van der Hulst and Sancisi 1988) showed that there are numerous holes in the HI distribution in the main disk. In addition, HI gas was detected at velocities not corresponding to the disk rotation, indicating the possible presence of the equivalence with the Galactic high velocity clouds (HVCs),

either due to accretion of fresh gas, or a collision with remnant gas clouds related to a tidal interaction event between this galaxy and a smaller neighbour. Deeper HI images of edge-on galaxies also became available, in particular for the galaxy NGC 891 (cf. Fig. 8). The observations of this very actively star forming galaxy show a thick HI disk (Swaters et al. 1997), and yet more sensitive data show a more extensive thick HI disk and a streamer (Oosterloo et al. 2007).

The main result for the thick HI disk in NGC 891 is that its rotation rate is lagging with respect to the thin disk, as already shown by Swaters et al. (1997), and more extensively in Fraternali et al. (2005). In Oosterloo et al. (2007) more modelling of NGC 891 was done, with a catalogue of possibilities: a thin disk, a strong warp along the line of sight, a flaring disk, a disk and corotating halo, a lagging halo with constant gradient, a lagging halo with high velocity dispersion, a lagging halo with a radial inflow motion, and a lagging halo with velocity gradient increasing in the inner parts.

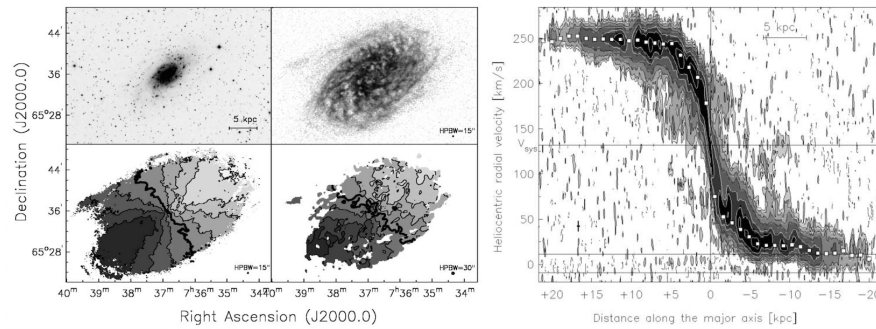


**Fig. 9** VLA observations of the galaxy NGC 2403 (reproduced with permission from Fraternali et al. 2001). *Left* panel of four: *top*: Optical image from the Digital Sky Survey (*left*) and HI distribution (*right*) of the main disk component; *bottom*: velocity field of the main disk component (*left*) and of the anomalous gas component (*right*). *Right* panel: position-velocity diagram along the major axis, clearly showing the anomalous velocities (the “beard”). The derived rotation curve of the main disk component is superimposed, and the lines at the bottom of the plot show the range of velocities where contamination by galactic emission was filtered out

It was realized that there could also be an effect of lagging HI halo gas seen in the observations of more face-on galaxies. Indeed, a position-velocity diagram for the galaxy NGC 2403 (Fraternali et al. 2001, 2002; Fig. 9) shows that there is an anomalous component with  $\sim 10\%$  of the total HI mass. The rotation velocity of the anomalous gas is  $25 - 50$  km/s lower than that of the disk. Its velocity field has non-orthogonal major and minor axes implying an overall inflow motion of  $10 - 20$  km/s toward the centre of the galaxy. A similar phenomenon is also seen in the THINGS observations of the galaxy NGC 3198 shown in Fig. 11 (upper panel), and is better brought out by the deeper imaging of this galaxy by Gentile et al. (2013), who find that  $\sim 15\%$  of the total HI gas mass is in a thick disk with a scale height of about  $3 \pm 1$  kpc.

Fraternali and Binney (2006) explored an initial model, where galactic fountain activity leads to clouds being sent up in the halo, and then falling back to the disk again, but this did not explain the lagging of the rotation of the extraplanar gas, nor the inflow towards the disk. Sancisi et al. (2008), in a review, discuss the signatures of HI gas accretion around nearby galaxies, and found an average visible HI accretion rate of  $\sim 0.2 M_{\odot} \text{ year}^{-1}$ . This is an order of magnitude too low to sustain the current star formation rates in some of the galaxies studied. Fraternali and Binney (2008) improved their galactic fountain model by considering the interaction of the fountain clouds with the hot coronal gas in the halo, the presence of which is expected theoretically, and ought to be observable in X-ray observations (see Hodges-Kluck and Bregman 2013 for a detection of that gas in NGC 891). A higher accretion rate can then be obtained, which is more of order of the star formation rate, so that the latter could be sustained from infalling gas over a longer timescale (e.g., Fraternali 2014, and references therein). For a recent in-depth review of this accretion model, see Fraternali (2016).

To follow up on this, the HALOGAS project was undertaken with the WSRT, but, while first results have been published, a conclusive paper has still to be completed. From presentations at conferences, it appears that NGC 891 is a relatively rare case, given its active star formation and extensive extraplanar gas distribution, which has been detected at other wavelengths as well (e.g., radio continuum: Allen et al. 1978, H $\alpha$ : Rand et al. 1990, X-ray: Hodges-Kluck and Bregman 2013). Dahlem et al. (2006) argue on the basis of several examples that the presence of radio continuum thick disks is correlated with active star formation.

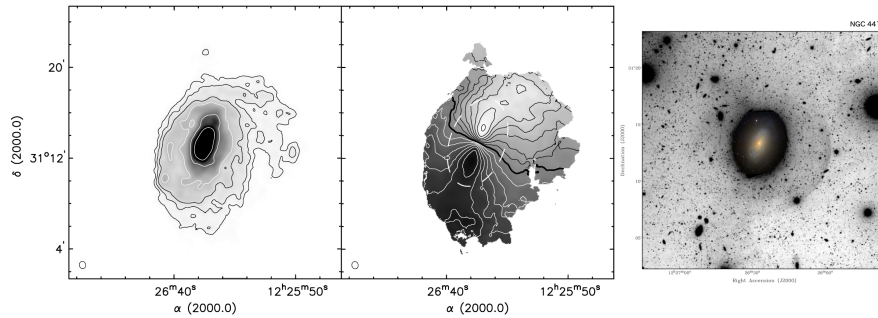


**Fig. 10** Deep HI imaging of the galaxy NGC 4414 (reproduced with permission from de Blok et al. 2014a). From *left to right*, the HI image, with the outer column density contour being  $2 \times 10^{19} \text{ cm}^{-2}$ , the velocity field indicating a strong warp in the northwestern part of the galaxy, and a deep optical image showing an outer shell feature, with a colour SDSS image overlaid in the inner parts. The outer isophotes of the SDSS image have a lower axial ratio than those of the outer isophotes of the main galaxy body in the deeper image

Several HALOGAS case studies have been published. New data on NGC 4414 (de Blok et al. 2014a) show that the outer warped HI layer is dynamically somewhat offset from the central parts, while on a deep optical image a shell structure is

seen in the western part. Both the warp and the thickening of the main galaxy (the inclination is higher in the central parts of the galaxy than the outline of the main galaxy body seen in Fig. 10) could be due to an interaction which caused also the shell structure itself.

Concurrently, the HALOGAS galaxies were observed with the Green Bank Telescope (GBT), to look for further HI gas at lower column densities. de Blok et al. (2014b) found a cloud near NGC 2403 in the GBT data, which has an HI mass of  $4 \times 10^6 M_{\odot}$  which is 0.15% of the total HI mass of the galaxy. It seems to link up with a  $\sim 10^7 M_{\odot}$  filament in the anomalous HI gas described in Fraternali et al. (2002). Likewise, Heald (2015) report about a few HVC like clouds with a total HI mass of  $4 \times 10^6 M_{\odot}$  around NGC 1003. The very low column density HI filament between M31 and M33 discovered by Braun and Thilker (2004) was reobserved by Wolfe et al. (2013), and shown to be composed for  $\sim 50\%$  of discrete clouds, embedded in more diffuse gas. To conclude, it can be said that there is HI around disk galaxies which could be accreted, but the amount of mass is not enough to sustain the star formation rate in the main disk (cf. Heald 2015).

This gas accretion problem has almost completely superseded the attention given to the flaring of the HI gas layer. Allaert et al. (2015) have taken the latter problem up again, and find that the HI disk in NGC 5907 is flaring, while they do not exclude a moderate flaring for other edge-on galaxies. Kalberla and Dedes (2008) show a significant flaring for the gas disk of the Milky Way, in agreement with earlier studies. Note that although a lot of modelling of the stellar disk of edge-on galaxies has been done assuming no flaring, the work by Saha et al. (2009) and Streich et al. (2016) shows evidence for a mild flaring of the older stellar disk in a number of edge-on galaxies.

#### ***6.4 Velocity Dispersions in the Outer HI Layers of Spiral Galaxies***

As discussed at the start of this Section, the flaring problem depends in part on the determination of the vertical velocity dispersion of the HI gas, and early work with the WSRT indicated a value around 10 km/s, with a slight enhancement in star forming regions as found for NGC 628 by Shostak and van der Kruit (1984). Dickey et al. (1990) determined that for NGC 1058 the velocity dispersion in the gas outside the optical image is remarkably constant at 6 km/s. Further work on this was done by Kamphuis (1993) and Kamphuis and Sancisi (1993), in particular for the relatively face-on galaxy NGC 6946, where the velocity dispersion was determined after derotating the data cube by resetting the intensity-weighted mean velocities of the individual profiles to the same central velocity before adding them, as suggested already by Boulanger and Viallefond (1992). It was shown more clearly that the higher velocity dispersions are related to star formation activity.

In the framework of the THINGS project, Tamburro et al. (2009) determine HI gas velocity dispersions for 11 galaxies, and found again evidence for lower velocity dispersions in the extended HI envelopes beyond the optical image and high

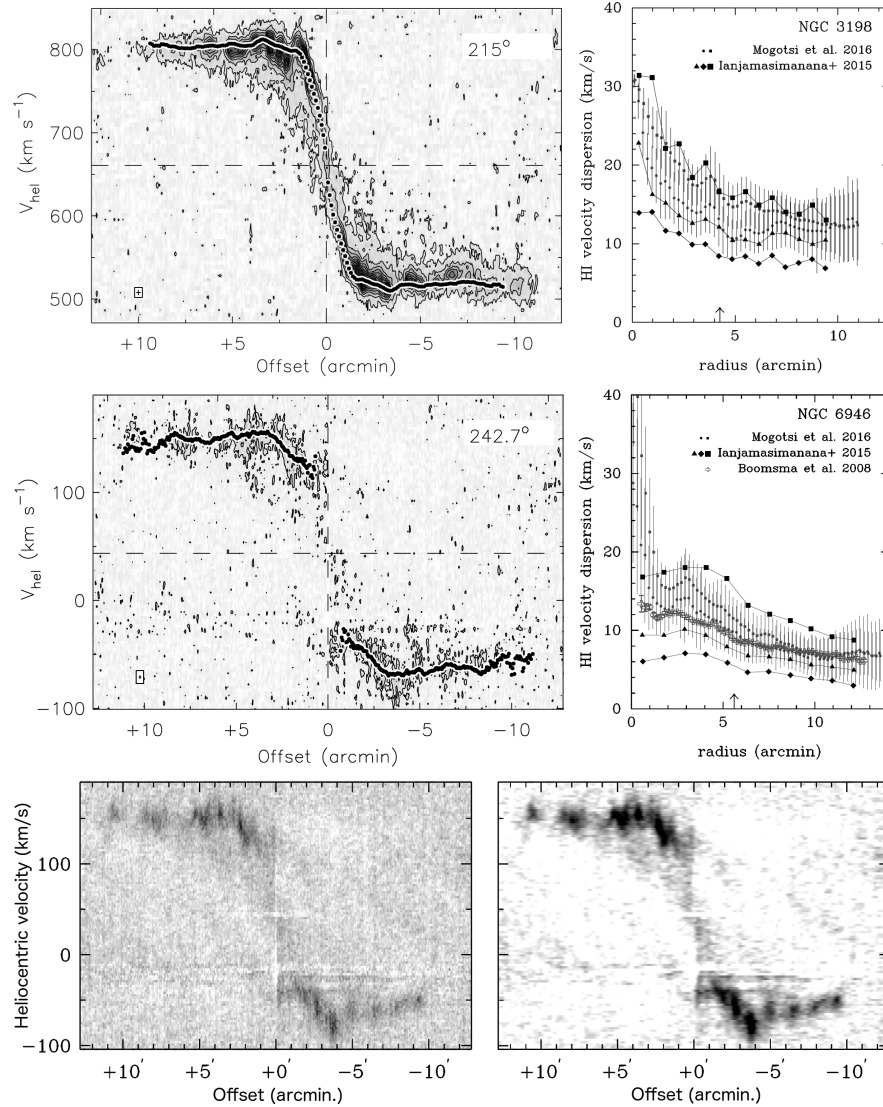


**Fig. 11** *Top*: Position-velocity diagram along the major axis of NGC 3198 (reproduced with permission from de Blok et al. 2008, *left*), and various radial profiles of the HI gas velocity dispersion (*right*). *Middle*: idem for NGC 6946. *Bottom*: Position-velocity diagrams along the major axis of NGC 6946, using the available data cube from NED: at left the data with beam size of 6''0 × 5''6, and at right the 18''0 × 18''0 data. The “beard” shows up rather well in the smoothed data. The horizontal stripes are due to incomplete subtraction of galactic foreground emission

velocity dispersions in the inner parts of actively star forming galaxies. If correct, the model calculation in Fig. 7 (right panels) suggests that a gradient in the velocity

dispersion from, e.g., 10 to 6 km/s, as seen in several cases, can lead to the absence of significant flaring.

There are various ways to go about the determination of the HI gas velocity dispersion, and Tamburro et al. (2009) took the simplest way, i.e., considering the second moment map derived from the profiles in the data cube. However, various geometric effects need to be taken into account. One is that the HI might not be a single layer, but in a combination of a low velocity dispersion thin disk and a higher velocity dispersion thick disk. This has been taken up recently for a number of galaxies in the THINGS sample (Ianjamasimanana et al. 2012, 2015; Mogotsi et al. 2016). The results for NGC 3198 are shown in Fig. 11, side by side with the position-velocity diagram along the major axis. This galaxy does not have the most favourable orientation for this work (perhaps too edge-on), but the results are illustrative of the difficulties involved. Ianjamasimanana et al. (2015) use “super-profiles”, i.e., profiles corrected for the effect of rotation, and stacked in annuli  $0.2R_{25}$  wide. They fit both a double Gaussian to low- and high-velocity components, as well as a single Gauss fit which allows comparison with older data in the literature. The low-velocity component is thought to represent the cold neutral medium in the thin HI disk, and the higher-velocity component the warm neutral medium in a thicker disk. Mogotsi et al. (2016) present in an Appendix the results from fitting a single Gaussian to the profiles as well as taking the second moment. The comparison in Fig. 11 shows that the results differ widely. In the very central parts, the data are influenced by the broadening of the profiles inside a spatial resolution element (i.e., beam smearing). Outside, there is a large difference between the second moment and a Gaussian fit, on account of the skewness of the profiles. As discussed already in Sect. 6.3, for NGC 3198, this skewness is due to the presence of a thick disk with lagging rotation (Gentile et al. 2013).

For the more face-on galaxy NGC 6946, the results from both studies also show again the presence of a low- and high-velocity dispersion component. Older WSRT data by Boomsma et al. (2008) show an HI velocity dispersion profile similar to the one found in Kamphuis (1993), and the profile determined by Gaussian fitting of Mogotsi et al. (2016) agrees reasonably well with this. However, the single Gauss fit by Ianjamasimanana et al. (2015) is definitely lower, presumably due to the selection of only profiles with signal-to-noise ratio of three or more to be included into the stacked profiles. What is most striking, however, is that the velocity dispersions in NGC 6946 are lower than those in NGC 3198, despite the fact that NGC 6946 is forming stars more actively. The difference is perhaps due to the presence of more extraplanar gas in NGC 3198. Moreover, NGC 3198 is seen relatively edge-on, so there are line of sight integration effects. However, analysis of the publicly available data cube of NGC 6946 suggests another cause: if I smooth the cube from  $6''.0 \times 5''.6$  to  $18''.0 \times 18''.0$ , the “beard” shows up in the smoothed version of the position velocity diagram (cf. Fig. 11, lower panels). Thus considerations of spatial resolution and sensitivity, as well as the spatial orientation of the galaxy with respect to the line of sight all play a role in the outcome of the studies of this problem. And, of course, if the question is asked: “what about the magnetic field?”, it is strong in NGC 6946, and much weaker in NGC 3198. Beck (2007) shows that in the outer

parts of NGC 6946 the magnetic field energy density is higher than the energy in turbulent motions, so this cannot be neglected in the calculations of the thickness of the gas layer, at least for that galaxy.

### 6.5 Star Formation in Warped HI Layers

Occasionally, star formation is seen in the warped HI layers, as in, e.g., NGC 3642 (Verdes-Montenegro et al. 2002), where the outer disk of low surface brightness has a different spatial orientation than the inner parts. This galaxy was later taken as a prototype of a Type III radial surface brightness profile in Laine et al. (2014), i.e., having an exponential disk with in the outer parts an upbending profile. This situation is noted also for Malin 1 (see also Sect. 3). van der Kruit (2007) notes that for the survey of warps in edge-on galaxies by García-Ruiz et al. (2002), the onset of the warp is rather abrupt, and occurs, for most of the galaxies considered, just outside the truncation radius if there is one. However, faint star forming regions can be found in a number of XUV disks, as shown in Fig. 5 (lower left) for NGC 5055 and Fig. 7 (top, second panel from left) for NGC 3198. Koribalski and López-Sánchez (2009) present HI observations of the NGC 1510/1512 system, and state that the faint disk of NGC 1512, which contains strong spiral features, is warped with respect to the inner disk. Radburn-Smith et al. (2014) find that in the warped HI disk of NGC 4565, the young stellar populations participate in the warp, but not the older ones. Detection of molecular gas in some of these galaxies is discussed in Koda and Watson (this volume).

## 7 The Core-Cusp Problem

The  $\Lambda$ CDM theory of galaxy formation and evolution predicts that in dark matter-dominated galaxies the tracers of the potential should indicate a cuspy NFW profile (Navarro et al. 1996, 1997). However, this has not been observed, as already remarked by Moore (1994) and Flores and Primack (1994). Observations of late-type low surface brightness disk galaxies were done by a number of groups, first in HI, and later augmented with long-slit  $H\alpha$  observations in the inner parts (e.g., de Blok et al. 2001; de Blok and Bosma 2002; de Blok et al. 2003). These confirmed the presence of cores in such galaxies, or, at the most, mildly cusp slopes with  $\alpha = -0.2 \pm 0.2$ , not compatible with the NFW profiles. These results were (e.g., Swaters et al. 2003) and still are the subject of intense debate. CO and three-dimensional  $H\alpha$  observations (Simon et al. 2003, 2005; Blais-Ouellette et al. 2004; Kuzio de Naray et al. 2006, 2008) were also brought to bear on this problem. A review has been given in de Blok (2010).

Projects such as THINGS, and LITTLE THINGS, using HI observations at higher resolution and sensitivity, keep finding cores (Oh et al. 2008, 2011, 2015).

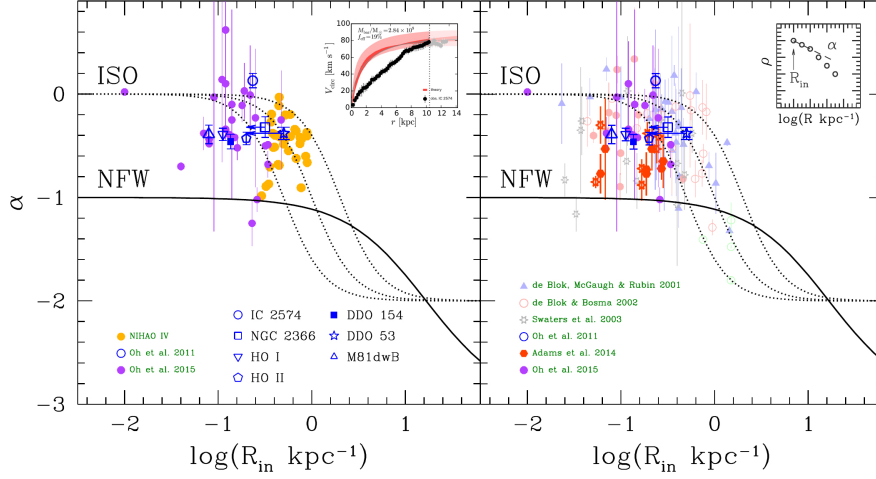


**Fig. 12** *Left*: results from Oh et al. (2011, 2015) for the slope of the dark matter density profile as function of the radius of the innermost point on the rotation curve. The orange points are from hydrodynamical zoom simulations from the NIHAO project (Tollet et al. 2016, their Fig. 13). The inset shows the current data for IC 2574 and the APOSTLE simulation result for it (reproduced with permission from Oman et al. 2016). *Right*: a similar plot which collects older data (de Blok et al. 2001; de Blok and Bosma 2002; Swaters et al. 2003), the data from Oh et al. (2011), data based on stellar and gas velocity dispersions (Adams et al. 2014), and the selected data for 15 galaxies from Oh et al. (2015) as described in the text. The dotted lines converging on  $\alpha = 0$  represent the theoretical variations in slope for ISO haloes with  $R_C = 0.5, 1$  and  $2$  kpc. The line converging on  $\alpha = -1$  shows the variation in slope for  $c/V_{200} = 8.0/100$

These observations can now be compared with modified predictions of the  $\Lambda$ CDM theory of galaxy formation and evolution, where star formation and feedback have been added to the ingredients (“subgrid physics”) of the numerical simulations. The results are given in Fig. 12, together with the results from cosmological zoom simulations of the NIHAO project (Tollet et al. 2016). The addition of baryonic physics changes the prediction for the dark matter profile towards a slope shallower than the NFW profile. However, the current resolution achieved in the NIHAO project does not yet probe the full range in inner radii comparable to those of the observations. The debate is ongoing about whether the  $\Lambda$ CDM theory should be further revised to accommodate the new observational results. I select here a couple of issues which can be addressed with HI data in the context of galaxy outskirts.

Oman et al. (2015, 2016) emphasize that there is a large variety in the data of late-type low surface brightness dwarfs, and find that the observations of the rotation properties of some dwarfs are closer to their models than others. They suggest that observers somehow do not have the systematics of galaxy inclinations under control. Read et al. (2016) claim good agreement with  $\Lambda$ CDM by discarding half their sample of four galaxies: IC 1613 is thought to be in disequilibrium due to starburst activity, and for DDO 101 the distance is too uncertain.

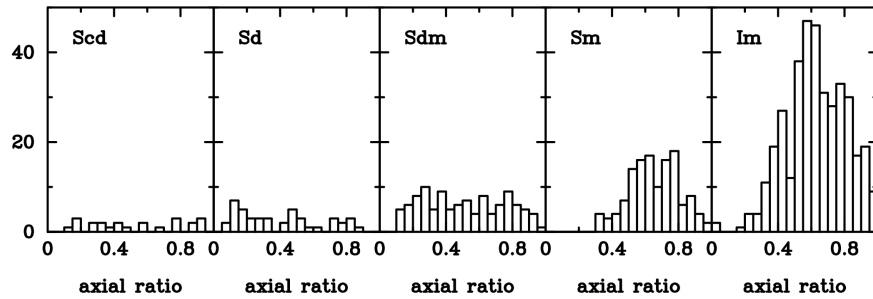


**Fig. 13** Statistics of axial ratios for late-type galaxies (numerical Hubble type  $\geq 6$ ) in the Local Volume Galaxy catalogue (Karachentsev et al. 2013), split out by morphological type

To examine the problem further, I looked at some of the underlying assumptions in the modelling of the observational data. One is that galaxy disks are thin, with a typical vertical axial ratio of 0.2. Such a value can be checked statistically, as has been done in the exemplary work of Sandage et al. (1970). For data in the Second Reference Catalog of Bright Galaxies (de Vaucouleurs et al. 1976), Binney and de Vaucouleurs (1981) point out that for Hubble types close to the end of the sequence (type 10), the distribution of apparent axial ratios does not indicate flattened disks. This was discussed further in Bosma (1994), and is illustrated here again in Fig. 13, now using data from the Local Volume Galaxy catalogue (Karachentsev et al. 2013), split by morphological type for the later types. While Scd, Sd and Sdm galaxies have histograms that seem compatible with those for flattened disks viewed from different orientation angles, the data for Sm and in particular Im galaxies show an apparent axial ratio distribution not compatible with this. It is thus likely that some of the dwarf galaxies used in the core-cusp debate are not modelled correctly when it is assumed that they are thin disks: instead, models with a considerable thickness should be explored. The results from the FIGGS sample (Begum et al. 2008; Roychowdhury et al. 2010) confirm this, and show that the thickness of the HI maps peaks around 0.5. Roychowdhury et al. (2013) also analyze the Local Volume catalogue, and find a similar thickening of the galaxies of later type, but their analysis considers only a few bins. As discussed further in Sect. 9.2, thick HI disks have been recognized as such by Puche et al. (1992), and even earlier by Bottema et al. (1986).

In Fig. 14 I use data from the recent collection of rotation curves studied by Lelli et al. (2016) concerning the mean velocity in the outer parts,  $V_{\text{flat}}$ , if defined. For the thin disk galaxies of type Sd and Sdm (numerical Hubble type 7 and 8) the range in  $V_{\text{flat}}$  overlaps the one of the thicker disk galaxies of type Sm, Im and BCD (types 9, 10 and 11, resp.). There is thus more to a galaxy than just its rotation curve, since the three-dimensional morphology of a galaxy does not follow automatically from the one-dimensional rotation curve. Therefore, for galaxies with  $V_{\text{flat}}$  between 70 and 110 km/s, corresponding to a stellar mass range of  $\sim 5 \times 10^8 - 4 \times 10^9 M_{\odot}$ , numerical simulations of galaxy formation and evolution ought to reproduce a variety of shapes

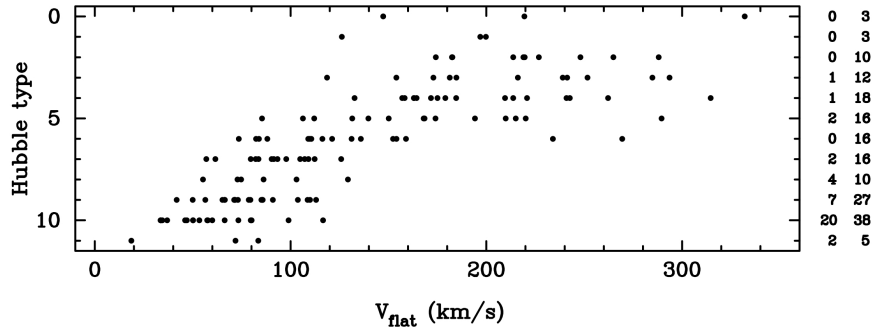


**Fig. 14** Statistics of the  $V_{\text{flat}}$  value from the SPARC sample (Lelli et al. 2016) split out by morphological type. The number of galaxies not reaching a  $V_{\text{flat}}$  value, and the total number per type bin, are indicated at the right. Note the overlap in  $V_{\text{flat}}$  for types 7 – 10

in the stellar mass distribution, rather than a single one, and for smaller galaxies a thicker stellar disk should be produced.

I further consider the data on the LITTLE THINGS project discussed by Oh et al. (2015). In that paper, the HI layer is assumed to be infinitesimally thin, and the thickness of the stellar component is computed from the ratio of disk scale length to disk scale height ( $h/z_0$ ) of 5.0, which holds for large spiral galaxies seen edge-on, but not necessarily for dwarfs. To minimize problems, I selected only galaxies for which the difference in position angle and inclination derived from the HI data and those from the axial ratio of the optical images, as given in Hunter et al. (2012), is less than 25 degrees (as  $\sqrt{\Delta(\text{PA})^2 + \Delta(\text{Inc})^2}$ ). This leaves 15 galaxies, which are shown in Fig. 12 (right panel). Selecting “better behaving” dwarf galaxies, with little warping of the HI disk, thus does not alleviate the core-cusp problem. A more elaborate analysis is beyond the scope of this review.

## 8 Alternative Gravity Theories

A recurrent issue with the interpretation of HI rotation curves is the argument that the dark matter interpretation is not necessarily correct, starting with a paper by Milgrom (1983) proposing MOND (“MODified Newtonian Dynamics”). Begeman et al. (1991) made models for 10 galaxies, both for Newtonian gravity and for MOND, and pointed out that a common critical acceleration parameter can be found once some leeway is allowed for galaxy distances. Reviews about MOND and its relative success in reproducing rotation curves have been produced by Sanders and McGaugh (2002) and Famaey and McGaugh (2012). However, the applicability of MOND to larger scales, such as clusters of galaxies, is problematic, and Angus (2009) argues for the presence of 11 eV neutrinos to cure this. Such particles have not been found yet, but then, the nature of the dark matter remains unknown.

The fate of the Vulcan hypothesis by Le Verrier (cf. Fontenrose 1973) is frequently quoted to illustrate the idea behind MOND (modifying the theory of gravity rather than searching for additional planets), but the history of dark matter detection resembles now more the discovery story of Pluto, rather than of Neptune.

My own contribution to this has been limited to refereeing some of the papers, and I will neither treat the debate here, nor discuss other alternative theories. What is of interest are the attempts to disprove MOND, by emphasizing the discrepancies with HI imaging data. There are manifest problems with some galaxies if their Cepheid distance is adopted, the clearest case being NGC 3198 (cf. Bottema et al. 2002; Gentile et al. 2011, 2013). For late-type dwarf galaxies, the recent results of Carignan et al. (2013) for NGC 3109, and Randriamampandry and Carignan (2014) for DDO 154, IC 2574, NGC 925 and NGC 7793—in addition to NGC 3109 and NGC 3198—clearly bring out discrepancies as well. However, Angus et al. (2012) could reduce the discrepancy for DDO 154 by considering a thick gaseous disk, up to the point of getting a reasonable fit for most of the radial extent of this galaxy. Such thick HI gas disks are not unreasonable for DDO 154 and IC 2574, in view of the discussion above, in Sect. 7, and further in Sect. 9.2, but less so for the Sd galaxies NGC 925 and NGC 7793. Finally, the often cited “dip” in the rotation curve of NGC 1560 (Broeils 1992; Gentile et al. 2010) poses a problem, since the curve determined from the data for the northern half of this galaxy does not have a dip, while the one for the southern part does, due to a local absence of gas and stars there; the mean thus has “half a dip”!?

MOND does not go away easily, and the recent result from 153 galaxies in the SPARC sample (12 galaxies too face-on and 10 galaxies too asymmetric were rejected, cf. McGaugh et al. 2016), i.e., a tight relation, with a scatter of  $\sim 30\%$  on a log-log plot, of the acceleration determined from rotation curves compared to the one based on  $3.6\ \mu\text{m}$  radial surface brightness profiles assuming a constant  $M/L$ -ratio for galactic disks, revived some interest in it. Ludlow et al. (2016) argue that the small scatter in this mass-discrepancy - acceleration relation is due to different feedback processes moving data points along this line, rather than deviating strongly from it, so that the  $\Lambda\text{CDM}$  theory does not have much difficulty explaining it. However, this leaves the core-cusp problem unsolved (cf. Fig. 12, inset of left panel).

The diversity of the  $3.6\ \mu\text{m}$  radial surface brightness profiles (e.g., Type I, II and III profiles—Martín-Navarro et al. 2012; Muñoz-Mateos et al. 2013; Kim et al. 2014; Laine et al. 2014), and the various physical processes invoked to explain these down- or up-bending profiles, cannot be ignored. Furthermore, in Famaey and McGaugh (2012), the two galaxies presented as examples for good MOND fits, NGC 6946 and NGC 1560, have a different  $K$ -band  $M/L$ -ratio (0.37 vs 0.18), i.e., a factor of two difference, which is just the order of magnitude difference discussed in Sect. 5. Moreover, data from the high angular resolution THINGS and LITTLE THINGS samples are not included in the SPARC sample, since, according to Lelli et al. (2016), their rotation curves are characterized by many small-scale bumps and wiggles thought to be due to non-circular components such as streaming motions along spiral arms. This exclusion is ironic, seen that when MOND is discussed, the capacity of reproducing such bumps is deemed very important. Anyway, these

“details” seem to operate on a different level of complexity than the overall mass-discrepancy - acceleration relation. Perusal of the individual mass models of each of the SPARC galaxies confirms this: the limiting surface brightness of the  $3.6\ \mu\text{m}$  profiles used in those mass models is  $23.8 \pm 1.8\ \text{mag arcsec}^{-2}$ , i.e., faint surface brightness levels are not considered for every galaxy.

## 9 Irregular Galaxies

### 9.1 Very Large HI Envelopes

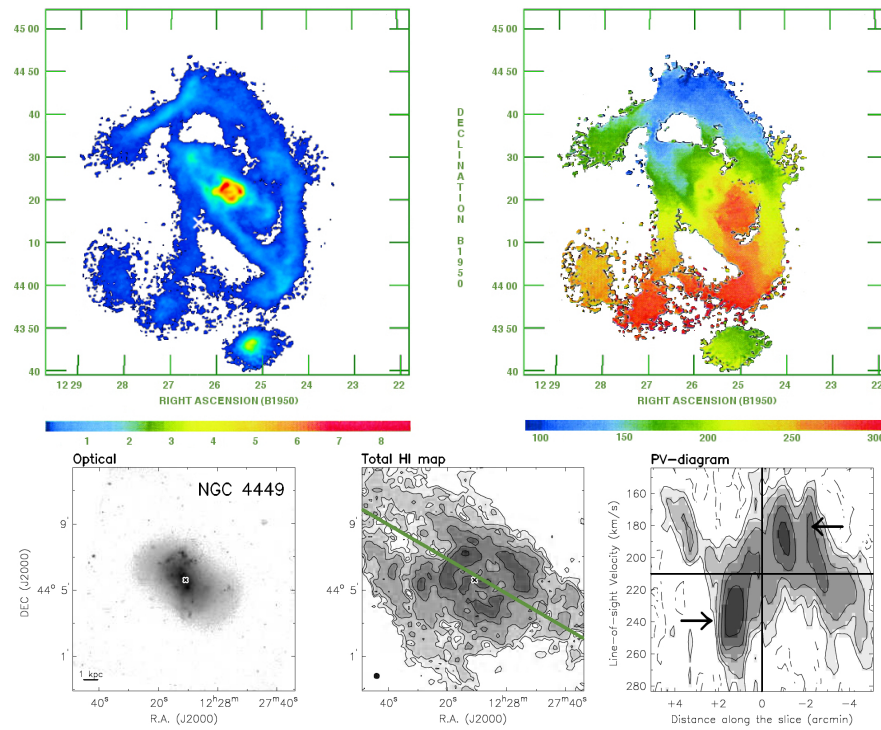


**Fig. 15** *Top*: HI image (*left*) and velocity field (*right*) of the Magellanic irregular galaxy NGC 4449 (adapted with permission from Hunter et al. 1998). The southernmost blob is the companion galaxy DDO 125. The cross is the position of the stellar stream as given in Rich et al. (2012). *Bottom*: details of the central parts of this galaxy (reproduced with permission from Lelli et al. 2014): a V-band optical image (*left*), the HI image (*centre*), and a position-velocity diagram (*right*) at a position angle of  $60^\circ$  along the green line indicated in the HI image showing the inversion of the line-of-sight velocities in the inner parts

Irregular galaxies can be intriguing, as is shown by observations of the giant magellanic irregular galaxy NGC 4449, whose stellar mass is  $1.8 \times 10^9 M_{\odot}$  (Muñoz-Mateos et al. 2015), i.e., 89% of that of NGC 300. A large HI envelope around this galaxy had already been discovered by van Woerden et al. (1975), using the 100 m Effelsberg telescope. A  $3 \times 3$ -point mosaic with the VLA of this galaxy has been made by Hunter et al. (1998). The small irregular galaxy DDO 125 is present as the southernmost blob in the images in Fig. 15. A further faint dwarf, or rather an extended stellar stream, discussed more recently by Rich et al. (2012), Martínez-Delgado et al. (2012) and Toloba et al. (2016), is indicated by a cross in the HI image: there is no immediate connection between this object and the HI features. The outer envelope shows a regular velocity gradient from north to south, while the body of the main galaxy seen in the visible light shows a regular velocity gradient at a position angle of  $\sim 60^{\circ}$  in the opposite sense. Lelli et al. (2014) remark that if for NGC 4449 the rotation velocity of the outer envelope is used this galaxy falls on the baryonic Tully-Fisher relation. This suggests that it is the outer envelope which traces the dark halo, and that the inner parts, including the visible galaxy, are not yet settled.

Galaxies with such large HI envelopes (more than five times larger than the optical radius) are relatively rare, and only a handful of other cases have been discussed. Blue compact dwarfs can sometimes be surprisingly large in HI, as is the case for NGC 2915, which has a relatively regular HI disk (cf. Meurer et al. 1996; Elson et al. 2010, 2011a,b, see Fig. 16, upper panels), UGC 5288 (van Zee 2004), NGC 3741 (Begum et al. 2005), ADBS 113845+2008 (Cannon et al. 2009), IZw18 (Lelli et al. 2014), and IIZw40 (Brinks and Klein 1988). Note that DDO154 also has a very large HI size compared to its optical size (Carignan and Freeman 1988; de Blok et al. 2008).

Some galaxies look a bit surprising, such as NGC 4214, shown in Fig. 16 (middle panels). If the HI is in a circular disk seen in projection, there is a large misalignment of  $\sim 55^{\circ}$  between the position angle of its major axis, and the one derived from the velocity field. Lelli et al. (2014) fit a tilted ring model to the observations of this galaxy, and derive a variable inclination, which tends to  $0^{\circ}$  in the outer parts. This seems hard to square with the apparent axial ratio of the HI distribution.

Also shown in Fig. 16 (lower panels) is the galaxy Holmberg II, imaged already by Puche et al. (1992), and later in the THINGS and VLA-ANGST projects. From the velocity field, a clear warp can be inferred, and the HI image also shows a tail towards the west side. Nevertheless, several analyses have been performed on this galaxy. One of the striking aspects in the HI distribution is the presence of holes, also discussed for bright galaxies, such as M101 by van der Hulst and Sancisi (1988), and NGC 6946 by Boomsma et al. (2008). Puche et al. (1992) remark that HI holes in late-type dwarf galaxies are larger than the HI holes in large spiral galaxies.

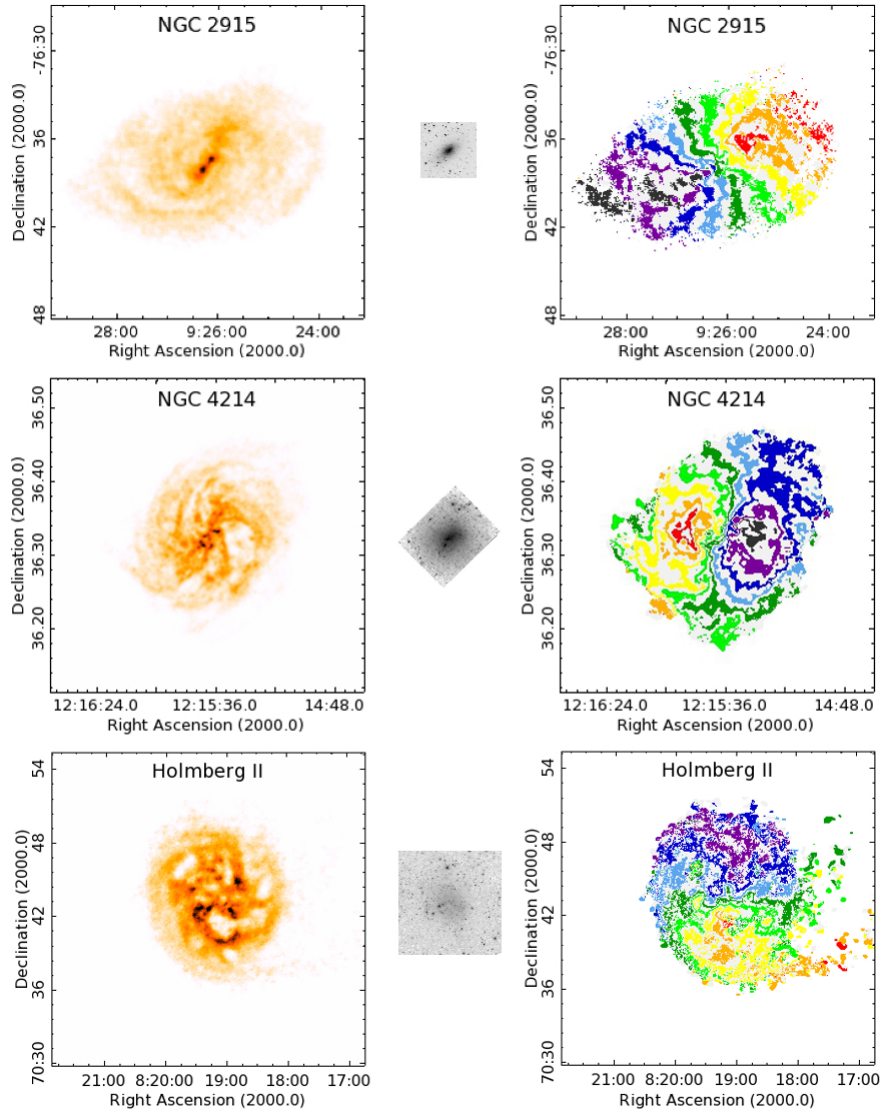


**Fig. 16** *Top:* HI image (*left*) and velocity field (*right*) of the blue compact dwarf NGC 2915, made from data kindly supplied by E. Elson, as reported in Elson et al. (2010). The 3.6  $\mu\text{m}$  image in the middle is on the same scale. *Middle:* HI image (*left*) and velocity field (*right*) of NGC 4214, from the THINGS project, and a 3.6  $\mu\text{m}$  image. *Bottom:* HI image (*left*) and velocity field (*right*) of Holmberg II, from the ANGST project, and a 3.6  $\mu\text{m}$  image. The THINGS, ANGST and 3.6  $\mu\text{m}$  data were downloaded from the NED

## 9.2 Velocity Dispersions in Dwarf Irregular Galaxies

A number of recent surveys concern almost uniquely dwarf irregular galaxies. In particular, the ANGST survey (Ott et al. 2012) has observed or re-observed a number of dwarfs with the VLA at high spectral resolution. An extensive discussion of HI gas velocity dispersions based on these observations is given in Stilp et al. (2013a,b). The dispersions have again been calculated on the basis of “super-profiles”, derived after derotating the data cube and stacking the individual profiles. The general shape of the profiles can be described by a double Gaussian, with a narrow centre of order 7.2 – 8.5 km/s and a wider wing of order 20 – 25 km/s. The latter is presumably due to the influence of star formation, while the former is attributed to turbulence. Stilp et al. (2013a) do not think it is possible to discriminate between the “cold neutral medium” (CNM) and the “warm neutral medium” (WNM), as done by Ianjamasimanana et al. (2012) for the THINGS data, since the typical velocity dispersions expected for the typical temperatures associated with these do not match. They also argue that the data cubes with robust weighting should be used, and that the signal-to-noise threshold matters.

Interestingly, thicknesses of the gas layer have been derived, based on a hydrostatic equilibrium used already in Ott et al. (2001) and even before that by Puche et al. (1992). Banerjee et al. (2011) studied the flaring of the gas layer in four of the THINGS dwarf galaxies, again using the hydrostatic equilibrium approach. For DDO 154, the disk flares to  $\sim 1$  kpc at a radius of  $\sim 5$  kpc. This is to be compared with an overall thickness derived by Stilp et al. (2013b) of  $708 \pm 139$  pc based on the method discussed by Ott et al. (2001), and a thickness of 650 pc calculated by Angus et al. (2012) to get a more or less acceptable MOND fit (cf. Sect. 8). Very recently, Johnson et al. (2017) also argue that the HI disks in galaxies in the LITTLE THINGS survey are thick, rather than thin.

## 10 The Relation Between HI Extent and the Optical Radius

A specific search for galaxies large in HI has been executed by Broeils and van Woerden (1994) and Broeils and Rhee (1997), using short observations with the WSRT. Broeils and Rhee reported an interesting correlation between the HI mass and the HI size, the latter defined as an isophotal radius at the level of  $1 M_{\odot} \text{pc}^{-2}$ . More recently, a number of surveys have been executed on various telescopes, typically with sample sizes of order 10 – 60 galaxies. Wang et al. (2016) collected HI sizes as defined by Broeils and Rhee (1997) for 437 galaxies—spread over 14 projects—although not for every galaxy an HI size was determined, and there might be a slight overlap in the sense that several galaxies are in more than one sample. They found again a very tight relationship between the HI mass and the HI size. It is instructive to examine for each survey they considered the distribution of the ratio of HI to optical size, which is shown in Fig. 17. The survey done by Broeils and Rhee (1997) shows a peak at  $R_{\text{HI}}/R_{\text{opt}} \sim 1.5$ , and they found relatively few galaxies with

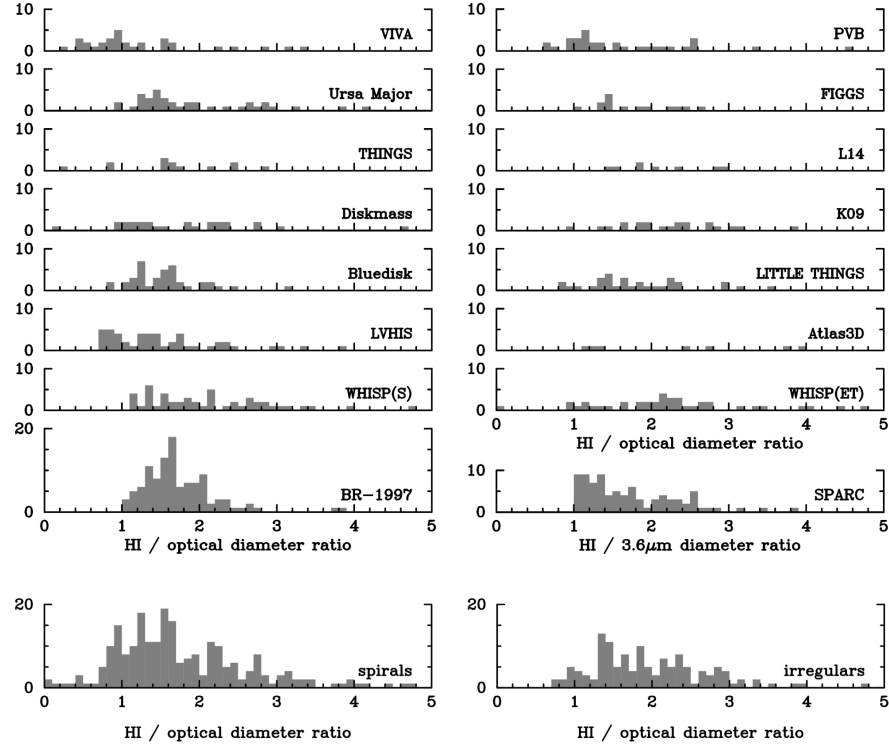


**Fig. 17** Statistics of the ratio of HI diameter, evaluated at  $\Sigma_{\text{HI}} = 1 M_{\odot} \text{pc}^{-2}$ , to the optical diameter, following Wang et al. (2016), except for the Bluedisk sample, for which Wang et al. (2013) data are used. The samples are: BR-1997—Broeils and Rhee 1997; WHISP(S)—Swaters et al. 2002; LVHIS—Koribalski 2008; Westmeier et al. 2011, 2013; Bluedisk—Wang et al. 2013; Diskmass—Martinsson et al. 2016; THINGS—Walter et al. 2008; Ursa Major—Verheijen and Sancisi 2001; VIVA—Chung et al. 2009; WHISP(ET)—Noordermeer et al. 2005; Atlas3D—Serra et al. 2012, 2014; LITTLE THINGS—Hunter et al. 2012; K09—Kovač et al. 2009; L14—Lelli et al. 2014; FIGGS—Begum et al. 2008; PVB—Ponomareva et al. 2016. Note that several large galaxies are missing from the LVHIS, THINGS, LITTLE THINGS, FIGGS and VIVA samples, while for the WHISP samples a maximum diameter of  $400''$  is imposed, on account of missing flux when comparing the interferometric data with single-dish observations or too large in extent compared to the primary beam. For the SPARC sample (Lelli et al. 2016) I determined the  $3.6 \mu\text{m}$  radius from the tables associated with their publication, by interpolating those radial luminosity profiles which reached a depth of  $1.0 L_{\odot} \text{pc}^{-2}$ , which could be done for 84 of the 174 galaxies in that sample. The *bottom* row refers to the total number of spirals (left) and irregulars (numerical Hubble type  $\geq 8.5$ , right) in the samples studied by Wang et al. (2016)

extended HI disks. The statistics based on the data by Wang et al. (2016) show that the proportion of extended HI disks is not too different for spirals compared to irregulars (even though statistically there are more irregulars with large  $R_{\text{HI}}/R_{\text{opt}}$ ), and the fraction of very extended disks with an HI size larger than, e.g., three times the optical size is about 10%.

Even though Broeils and Rhee (1997) found a very good relation between the HI mass and the size of the HI disk, indicating a roughly constant mean HI surface density, there is still no clear indication about when we can expect an HI disk which is much larger than the optical disk. This is due to the fact that the amount of HI in the extended HI disk is usually only a modest fraction of the total HI mass, so that differences are drowned in the “bigger things are bigger in many quantities” effect.

Not all surveys peak at the same HI-to-optical size ratio. This is to be expected for the Virgo cluster survey, VIVA (Chung et al. 2009), since in the centre of that cluster the HI gas in galaxy outskirts is subject to ram-pressure stripping against the hot intergalactic medium (IGM) probed by the X-ray emission. Indeed, several galaxies have been reported undergoing stripping, such as NGC 4522 (Kenney et al. 2004), NGC 4388, where a long HI tail has been observed (Oosterloo and van Gorkom 2005), NGC 4254 and its HI tail, including an HI dwarf almost devoid of stars (Minchin et al. 2007), and NGC 4569, where Boselli et al. (2016) report very extended H $\alpha$  emission.

Studies have shown that HI sizes of galaxies in a group environment could also be affected by the presence of the IGM. Obviously this is the case for compact groups (Verdes-Montenegro et al. 2001), where an evolutionary scenario is suggested depending on the state of the merging.

For loose groups, the effects are rather more subtle. In a recent extensive study, Wolfinger et al. (2016) analysed data for the Ursa Major region, and constructed a complete sample of 1209 galaxies limited in systemic velocity ( $300 \leq V_{\text{LG}} \leq 3000$  km/s), absolute magnitude ( $M_r \leq -15.3$ ) and stellar mass ( $M_* \geq 10^8 M_\odot$ ). They identified six groups with more than three members, centred around NGC’s 4449, 4258, 4278, 4026, 3938 and 5033, while 74% of the galaxies in their sample reside outside those groups. The high resolution interferometer data on the “Ursa Major cluster” (Verheijen and Sancisi 2001) and the CVn region (Kovač et al. 2009) are part of this sample, but for other parts of the region single-dish data from Jodrell Bank and Arecibo were used. There are HI-deficient galaxies associated with the densest parts of some of the groups, but not all, as, e.g., NGC 4449 (shown in Fig. 15), which does not seem HI-deficient. There are also galaxies with excess HI mass, usually in regions of low galactic density.

For the Sculptor group, Westmeier et al. (2011) find that the deep HI image of NGC 300 is asymmetric in the very outer parts, and attribute this to a possible interaction with the IGM in that group. The process of the formation of warps due to the interaction with the IGM has been explored further by Haan and Braun (2014). Deep HI imaging data on M83 with the KAT-7 telescope (Heald et al. 2016) shows sharp edges in the outer HI there as well, which can be either due to a ram pressure effect with respect to the surrounding IGM, or photoionisation, as discussed below.

The Void Galaxy Survey (Kreckel et al. 2011, 2012) investigated the properties of HI disks in galaxies in voids, and found that on average the statistics of the size ratio  $R_{\text{HI}}/R_{\text{opt}}$  are roughly similar to those observed by Swaters et al. (2002) for the late-type WHISP sample. The galaxy with the largest ratio, VGS\_12, has an HI disk in the polar direction of a small S0-like galaxy (cf. Stanonik et al. 2009). No star formation is associated with this HI gas. However, apart from this, there is nothing

outstanding about the properties of void galaxies with respect to the field galaxies studied in most other surveys.

The outermost HI is prone to be ionized by the ultraviolet background radiation, as already suggested by Sunyaev (1969). An early attempt to get limits on this has been done for NGC 3198 by Maloney (1993), using an unpublished deep VLA HI image. The realisation that there ought to be detectable ionized gas emission around HI envelopes, which could be used to probe the dark matter at larger radii, has led to some further studies of this gas using Fabry-Pérot  $H\alpha$  observations, but these are technically very challenging (cf. Bland-Hawthorn et al. 1997).

Hlavacek-Larrondo et al. (2011a,b) report deep  $H\alpha$  observations of three Sculptor group galaxies with the wide-field Fabry-Pérot system on the 36 cm Marseille Telescope in La Silla. For NGC 247, the  $H\alpha$  and HI data extend out to  $\sim 13.5$  arcmin, barely beyond the Holmberg radius of 12.2 arcmin. For NGC 300, the field of view was limited, and the region of the outer, warped HI disk not imaged in  $H\alpha$ . For NGC 253, the  $H\alpha$  disk goes out to similar radii (11.5 arcmin) as the HI disk seen with the VLA, but faint [NII] emission has been detected out to 19.0 arcmin at the southwest part of the galaxy. The kinematic data seem to indicate a declining rotation curve, but the galaxy is heavily perturbed there as seen on recent deep optical images, and recent KAT-7 HI data show the presence of extraplanar cold gas (Lucero et al. 2015). Earlier  $H\alpha$  observations of the Sculptor group galaxy NGC 7793 with the same instrument (Dicaire et al. 2008) led to the conclusion that the ionizing sources of the  $H\alpha$  disk of this galaxy are likely to be internal, rather than the UV background.

For more on the interface between the cold HI gas and the hotter circumgalactic medium, see the review by Chen (this volume).

## 11 Concluding Remarks

In this review, I have discussed a number of issues related to detailed HI imaging of the outskirts of nearby spiral and irregular galaxies done with current interferometers, such as the WSRT, the VLA, the ATCA and the GMRT. I have been selective in my topics, and avoided to discuss the issue of star formation in extended HI envelopes, since this is covered elsewhere in this volume. Most topics are related to the dark matter problem in one way or another. A number of results have been obtained by making case studies with the emphasis on improved sensitivity, rather than by simply observing more objects from a list.

The Square Kilometer Array project is advancing at great strides, and the associated approach of setting a challenging imaging target requiring the development of new instrumentation to reach it is soon going to bear fruit. Indeed, extensive HI imaging surveys of relatively nearby galaxies will start next year with SKA pathfinders, such as the WSRT Apertif survey, and the SKA precursors ASKAP (the WALLABY survey) and MeerKAT (the deep, targeted MHONGOOSE survey, and also the MALS survey). Some of the projects for the first phase of the SKA telescope,

SKA1, are described in the SKA science book (e.g., Blyth et al. 2015; de Blok et al. 2015). All these new surveys will bring fresh data of high quality, which can be brought to bear on the scientific problems discussed above and on other, related subjects, and will most likely lead to new insights and discoveries.

**Acknowledgements** I thank Lia Athanassoula for fruitful discussions and a careful reading of the manuscript. I also thank the editors for inviting me to write this review, and in particular Johan Knapen for his careful editing. I thank David Malin for sending me the deep image of M83 with the shallower image superimposed, and David Martínez-Delgado and Taylor Chonis for providing the image in the lower right panel of Fig. 5. Erwin de Blok supplied the script and Se-Heon Oh and Andrea Macciò supplied data for the construction of Fig. 12. Deidre Hunter helped out with Fig. 15. Ed Elson supplied the HI data on NGC 2915 from which I could make the top panel of Fig. 16. Jing Wang clarified an issue with the Bluedisk sample.

I acknowledge financial support from the People Programme (Marie Curie Actions) of the European Union's Seventh Framework Programme FP7/2007-2013/ under REA grant agreement number PITN-GA-2011-289313 to the DAGAL network, from the CNES (Centre National d'Etudes Spatiales - France), and from the "Programme National de Cosmologie et Galaxies" (PNCG) of CNRS/INSU, France. This research has made use of NASA's Astrophysics Data System. Use was made of the NASA/IPAC Extragalactic Database (NED) which is operated by the Jet Propulsion Laboratory, California Institute of Technology, under contract with the National Aeronautics and Space Administration to produce parts of Fig. 5, Fig. 7, Fig. 11 and Fig. 16.

## References

- Adams, J.J., Simon, J.D., Fabricius, M.H., et al. (2014), *ApJ*, 789, 63  
 Allaert, F., Gentile, G., Baes, M., et al. (2015), *A&A*, 582, A18  
 Allen, R.J., Sancisi, R., Baldwin, J.E. (1978), *A&A*, 62, 397–409  
 Angus, G.W. (2009), *MNRAS*, 394, 527–532  
 Angus, G.W., van der Heyden, K.J., Famaey, B., Gentile, G., McGaugh, S.S., de Blok W.J.G. (2012), *MNRAS*, 421, 2598–2609  
 Aniyani, S., Freeman, K.C., Gerhard, O.E., Arnaboldi, M., Flynn, C. (2016), *MNRAS*, 456, 1484–1494  
 Aparicio, A., Gallart, C. (2004), *AJ*, 128, 1465–1477  
 Arnaboldi, M., Oosterloo, T., Combes, F., Freeman, K.C., Koribalski, B. (1997), *AJ*, 113, 585–598  
 Athanassoula, E. (2002), *ApJL*, 569, L83–L86  
 Athanassoula, E. (2003), *MNRAS*, 341, 1179–1198  
 Athanassoula, E. (2008), *MNRAS*, 390, L69–L72  
 Athanassoula, E., Bosma, A., Papaioannou, S. (1987), *A&A*, 179, 23–40  
 Babcock, H.W. (1939), *Lick Observatory Bulletin*, 19, 41–51  
 Baldwin, J.E. (1974), In: Shakeshaft, J.R. (ed.) *The Formation and Dynamics of Galaxies*, IAU Symposium, vol 58, p. 139  
 Baldwin, J.E. (1975), In: Hayli A (ed) *Dynamics of the Solar Systems*, IAU Symposium, vol 69, p. 341  
 Banerjee, A., Jog, C.J., Brinks, E., Bagetakos, I. (2011), *MNRAS*, 415, 687–694  
 Barnabè, M., Dutton, A.A., Marshall, P.J., Auger, M.W., Brewer, B.J., Treu, T., Bolton, A.S., Koo, D.C., Koopmans, L.V.E. (2012), *MNRAS*, 423, 1073–1088  
 Beck, R. (2007), *A&A*, 470, 539–556  
 Becquaert, J.F., Combes, F. (1997), *A&A*, 325, 41–56  
 Begeman, K.G., Broeils, A.H., Sanders, R.H. (1991), *MNRAS*, 249, 523–537  
 Begum, A., Chengalur, J.N., Karachentsev, I.D. (2005), *A&A*, 433, L1–L4

- Begum, A., Chengalur, J.N., Karachentsev, I.D., Sharina, M.E., Kaisin, S.S. (2008), *MNRAS*, 386, 1667–1682
- Bershady, M.A., Andersen, D.R., Verheijen, M.A.W., Westfall, K.B., Crawford, S.M., Swaters, R.A. (2005), *ApJS*, 156, 311–344
- Bershady, M.A., Verheijen, M.A.W., Swaters, R.A., Andersen, D.R., Westfall, K.B., Martinsson, T. (2010a), *ApJ*, 716, 198–233
- Bershady, M.A., Verheijen, M.A.W., Westfall, K.B., Andersen, D.R., Swaters, R.A., Martinsson, T. (2010b), *ApJ*, 716, 234–268
- Bershady, M.A., Martinsson, T.P.K., Verheijen, M.A.W., Westfall, K.B., Andersen, D.R., Swaters, R.A. (2011), *ApJL*, 739, L47
- Bertone, G., Hooper, D. (2016), *ArXiv e-prints*, 1605.04909
- Binney, J., de Vaucouleurs, G. (1981), *MNRAS*, 194, 679–691
- Blais-Ouellette, S., Amram, P., Carignan, C., Swaters, R. (2004), *A&A*, 420, 147–161
- Bland-Hawthorn, J., Freeman, K.C., Quinn, P.J. (1997), *ApJ*, 490, 143–155
- Blyth, S., van der Hulst, J.M., Verheijen, M.A.W., et al. (2015), *Advancing Astrophysics with the Square Kilometre Array (AASKA14)*, 128
- Boomsma, R., Oosterloo, T.A., Fraternali, F., van der Hulst, J.M., Sancisi, R. (2008), *A&A*, 490, 555–570
- Boselli, A., Cuillandre, J.C., Fossati, M., et al. (2016), *A&A*, 587, A68
- Bosma, A. (1978) The distribution and kinematics of neutral hydrogen in spiral galaxies of various morphological types. PhD Thesis, Groningen University
- Bosma, A. (1981a), *AJ*, 86, 1791–1824
- Bosma, A. (1981b), *AJ*, 86, 1825–1846
- Bosma, A. (1994), *Kinematics and Dynamics of Dwarf Spirals and Irregulars*. In: Meylan G, Prugniel P (eds) *European Southern Observatory Conference and Workshop Proceedings, European Southern Observatory Conference and Workshop Proceedings*, vol 49, pp 187–196
- Bosma, A. (1999), *Dark Matter in Disk Galaxies*. In: Merritt DR, Valluri M, Sellwood JA (eds) *Galaxy Dynamics - A Rutgers Symposium, Astronomical Society of the Pacific Conference Series*, vol 182
- Bosma, A., van der Kruit, P.C. (1979), *A&A*, 79, 281–286
- Bottema, R. (1993), *A&A*, 275, 16
- Bottema, R. (1997), *A&A*, 328, 517–525
- Bottema, R., Shostak, G.S., van der Kruit, P.C. (1986), *A&A*, 167, 34–40
- Bottema, R., Pestaña, J.L.G., Rothberg, B., Sanders, R.H. (2002), *A&A*, 393, 453–460
- Boulanger, F., Viallefond, F. (1992), *A&A*, 266, 37–56
- Bovy, J., Rix, H.-W. (2013), *ApJ*, 779, 115
- Braun, R. (1997), *ApJ*, 484, 637–655
- Braun, R., Thilker, D.A. (2004), *A&A*, 417, 421–435
- Braun, R., Thilker, D.A., Walterbos, R.A.M., Corbelli, E. (2009), *ApJ*, 695, 937–953
- Briggs, F.H. (1990), *ApJ*, 352, 15–29
- Brinks, E., Klein, U. (1988), *MNRAS*, 231, 63p–67p
- Broeils, A.H. (1992), *A&A*, 256, 19–32
- Broeils, A.H., Rhee, M.H. (1997), *A&A*, 324, 877–887
- Broeils, A.H., van Woerden, H. (1994), *A&AS*, 107, 129–176
- Burbidge, E.M., Burbidge, G.R., Prendergast, K.H. (1960), *ApJ*, 131, 282
- Burbidge, G. (1975), *ApJL*, 196, L7–L10
- Burke, B.F. (1957), *AJ*, 62, 90
- Cannon, J.M., Salzer, J.J., Rosenberg, J.L. (2009), *ApJ*, 696, 2104–2114
- Carignan, C., Freeman, K.C. (1988), *ApJL*, 332, L33–L36
- Carignan, C., Frank, B.S., Hess, K.M., Lucero, D.M., Randriamampandry, T.H., Goedhart, S., Passmoor, S.S. (2013), *AJ*, 146, 48
- Chung, A., van Gorkom, J.H., Kenney, J.D.P., Crowl, H., Vollmer, B. (2009), *AJ*, 138, 1741–1816
- Courteau, S., Dutton, A.A. (2015), *ApJL*, 801, L20
- Dahlem, M., Lisenfeld, U., Rossa, J. (2006), *A&A*, 457, 121–131

- Dalton, G. (2016), In: Skillen, I., Barcells, M., Trager, S. (eds.) *Multi-Object Spectroscopy in the Next Decade: Big Questions, Large Surveys, and Wide Fields*, ASP Conference Series, vol 507, p 97
- Davies, R.D. (1974), In: Shakeshaft, J.R. (ed.) *The Formation and Dynamics of Galaxies*, IAU Symposium, vol 58, pp 119–128
- de Blok, E., Fraternali, F., Heald, G., Adams, B., Bosma, A., Koribalski, B. (2015), *Advancing Astrophysics with the Square Kilometre Array (AASKA14)*, 129
- de Blok, W.J.G. (2010), *Advances in Astronomy* 2010:789293
- de Blok, W.J.G., Bosma, A. (2002), *A&A*, 385, 816–846
- de Blok, W.J.G., McGaugh, S.S., Bosma, A., Rubin, V.C. (2001), *ApJL*, 552, L23–L26
- de Blok, W.J.G., Bosma, A., McGaugh, S.S. (2003), *MNRAS*, 340, 657–678
- de Blok, W.J.G., Walter, F., Brinks, E., Trachternach, C., Oh, S.H., Kennicutt, R.C. Jr. (2008), *AJ*, 136, 2648–2719
- de Blok, W.J.G., Józsa, G.I.G., Patterson, M., Gentile, G., Heald, G.H., Jütte, E., Kamphuis, P., Rand, R.J., Serra, P., Walterbos, R.A.M. (2014a), *A&A*, 566, A80
- de Blok, W.J.G., Keating, .K.M, Pisano, D.J., Fraternali, F., Walter, F., Oosterloo, T., Brinks, E., Bigiel, F., Leroy, A. (2014b), *A&A*, 569, A68
- de Vaucouleurs, G. (1958), *ApJ*, 128, 465
- de Vaucouleurs, G., de Vaucouleurs, A., Corwin, J.R. (1976), *Second reference catalogue of bright galaxies*, Austin: University of Texas Press
- Dicaire, I., Carignan, C., Amram, P., Marcelin, M., Hlavacek-Larrondo, J., de Denu-Baillargeon, M.M., Daigle, O., Hernandez, O. (2008), *AJ*, 135, 2038–2047
- Dickey, J.M., Hanson, M.M., Helou, G. (1990), *ApJ*, 352, 522–531
- Dutton, A.A., Treu, T., Brewer, B.J., Marshall, P.J., Auger, M.W., Barnabè, M., Koo, D.C., Bolton, A.S., Koopmans, L.V.E. (2013), *MNRAS*, 428, 3183–3195
- Efstathiou, G., Lake, G., Negroponte, J. (1982), *MNRAS*, 199, 1069–1088
- Einasto, J., Kaasik, A., Saar, E. (1974), *Nature*, 250, 309–310
- Elson, E.C., de Blok, W.J.G., Kraan-Korteweg, R.C. (2010), *MNRAS*, 404, 2061–2076
- Elson, E.C., de Blok, W.J.G., Kraan-Korteweg, R.C. (2011a), *MNRAS*, 411, 200–210
- Elson, E.C., de Blok, W.J.G., Kraan-Korteweg, R.C. (2011b), *MNRAS*, 415, 323–332
- Emerson, D.T., Baldwin, J.E. (1973), *MNRAS*, 165, 9P–13P
- Ewen, H.I., Purcell, E.M. (1951), *Nature*, 168, 356
- Faber, S.M., Gallagher, J.S. (1979), *ARAA*, 17, 135–187
- Famaey, B., McGaugh, S.S. (2012), *Modified Newtonian Dynamics (MOND): Observational Phenomenology and Relativistic Extensions*, *Living Reviews in Relativity*, 15
- Ferguson, A.M.N., Mackey, A.D. (2016), In: Newberg, H.J., Carlin, J.L. (eds.), *Astrophysics and Space Science Library*, vol 420, p 191
- Flores, R.A., Primack, J.R. (1994), *ApJL*, 427, L1–L4
- Fontenrose, R. (1973), *Journal for the History of Astronomy*, 4, 145–158
- Fragkoudi, F., Athanassoula, E., Bosma, A. (2016), *ArXiv e-prints*, 1605.05754
- Fraternali, F. (2014), In: Feltzing, S., Zhao, G., Walton, N.A., Whitelock, P. (eds.) *Setting the scene for Gaia and LAMOST*, IAU Symposium, vol 298, pp 228–239
- Fraternali, F. (2016), *Gas Accretion via Condensation and Fountains*. *ArXiv e-prints* 1612.00477
- Fraternali, F., Binney, J.J. (2006), *MNRAS*, 366, 449–466
- Fraternali, F., Binney, J.J. (2008), *MNRAS*, 386, 935–944
- Fraternali, F., Oosterloo, T., Sancisi, R., van Moorsel, G. (2001), *ApJL*, 562, L47–L50
- Fraternali, F., van Moorsel, G., Sancisi, R., Oosterloo, T. (2002), *AJ*, 123, 3124–3140
- Fraternali, F., Oosterloo, T.A., Sancisi, R., Swaters, R. (2005), In: Braun, R. (ed.), *Extra-Planar Gas*, *Astronomical Society of the Pacific Conference Series*, vol 331, p 239
- Freeman, K.C. (1970), *ApJ*, 160, 811
- Fuchs, B. (1999), In: Merritt, D.R., Valluri, M., Sellwood, J.A. (eds.), *Galaxy Dynamics - A Rutgers Symposium*, *Astronomical Society of the Pacific Conference Series*, vol 182, 365
- Galaz, G., Milovic, C., Suc, V., Busta, L., Lizana, G., Infante, L., Royo, S. (2015), *ApJL*, 815, L29

- García-Ruiz, I., Sancisi, R., Kuijken, K. (2002), *A&A*, 394, 769–789
- Gentile, G., Baes, M., Famaey, B., van Acoleyen, K. (2010), *MNRAS*, 406, 2493–2503
- Gentile, G., Famaey, B., de Blok, W.J.G. (2011), *A&A*, 527, A76
- Gentile, G., Józsa, G.I.G., Serra, P., Heald, G.H., de Blok, W.J.G., Fraternali, F., Patterson, M.T., Walterbos, R.A.M., Oosterloo, T. (2013), *A&A*, 554, A125
- Goad, J.W., Roberts, M.S. (1981), *ApJ*, 250, 79–86
- Gum, C.S., Kerr, F.J., Westerhout, G. (1960), *MNRAS*, 121, 132
- Haan, S., Braun, R. (2014), *MNRAS*, 440, L21–L25
- Heald, G. (2015), The Wsrst Halogas Survey. In: Ziegler, B.L., Combes, F., Dannerbauer, H., Verdugo, M. (eds.) *Galaxies in 3D across the Universe*, IAU Symposium, vol 309, 69–72
- Heald, G., de Blok, W.J.G., Lucero, D., Carignan, C., Jarrett, T., Elson, E., Oozeer, N., Randriamampandry, T.H., van Zee, L. (2016), *MNRAS*, 462, 1238–1255
- Hindman, J.V. (1967), *Australian Journal of Physics*, 20, 147
- Hlavacek-Larrondo, J., Carignan, C., Daigle, O., de Denus-Baillargeon, M.M., Marcelin, M., Epinat, B., Hernandez, O. (2011a), *MNRAS*, 411, 71–84
- Hlavacek-Larrondo, J., Marcelin, M., Epinat, B., Carignan, C., de Denus-Baillargeon, M.M., Daigle, O., Hernandez, O. (2011b), *MNRAS*, 416, 509–521
- Hodges-Kluck, E.J., Bregman, J.N. (2013), *ApJ*, 762, 12
- Hohl, F. (1971), *ApJ*, 168, 343
- Holmberg, E. (1958), *Meddelanden fran Lunds Astronomiska Observatorium Serie II*, 136, 1
- Hunter, D.A., Wilcots, E.M., van Woerden, H., Gallagher, J.S., Kohle, S. (1998), *ApJL*, 495, L47–L50
- Hunter, D.A., Ficut-Vicas, D., Ashley, T., et al. (2012), *AJ*, 144, 134
- Ianjamasimanana, R., de Blok, W.J.G., Walter, F., Heald, G.H. (2012), *AJ*, 144, 96
- Ianjamasimanana, R., de Blok, W.J.G., Walter, F., Heald, G.H., Caldu-Primo, A., Jarrett, T.H. (2015), *AJ*, 150, 47
- Johnson, M.C., Hunter, D.A., Kamphuis, P., Wang, J. (2017), *MNRAS*, 465, L49–L53
- Kahn, F.D., Woltjer, L. (1959), *ApJ*, 130, 705
- Kalberla, P.M.W., Dedes, L. (2008), *A&A*, 487, 951–963
- Kalnajs, A. (1983), Mass distribution and dark halos: Discussion. In: Athanassoula, E. (ed.) *Internal Kinematics and Dynamics of Galaxies*, IAU Symposium, vol 100, 87–88
- Kamphuis, J., Sancisi, R. (1993), *A&A*, 273, L31
- Kamphuis, J.J. (1993), *Neutral Hydrogen in nearby Spiral Galaxies: Holes and High Velocity Clouds*. PhD Thesis, University of Groningen
- Karachentsev, I.D., Karachentseva, V.E., Kudrya, Y.N., Sharina, M.E., Parnovskij, S.L. (1999), *The revised Flat Galaxy Catalogue*. *Bulletin of the Special Astrophysics Observatory* 47, astro-ph/0305566
- Karachentsev, I.D., Makarov, D.I., Kaisina, E.I. (2013), *Updated Nearby Galaxy Catalog*. *AJ*, 145, 101
- Kenney, J.D.P., van Gorkom, J.H., Vollmer, B. (2004), *AJ*, 127, 3361–3374
- Kent, S.M. (1986), *AJ*, 91, 1301–1327
- Kent, S.M. (1987), *AJ*, 93, 816–832
- Kent, S.M. (1988), *AJ*, 96, 514–527
- Kerr, F.J. (1957), *AJ*, 62, 93–93
- Khoperskov, S.A., Moiseev, A.V., Khoperskov, A.V., Saburova, A.S. (2014), *MNRAS*, 441, 2650–2662
- Kim T, Gadotti DA, Sheth K, et al. (2014), *ApJ*, 782, 64
- Koribalski, B.S. (2008), *Astrophysics and Space Science Proceedings*, 5, 41
- Koribalski, B.S., López-Sánchez, Á.R. (2009), *MNRAS*, 400, 1749–1767
- Kovač, K., Oosterloo, T.A., van der Hulst, J.M. (2009), *MNRAS*, 400, 743–765
- Kranz, T., Slyz, A., Rix, H.-W. (2003), *ApJ*, 586, 143–151
- Kreckel, K., Platen, E., Aragón-Calvo, M.A., van Gorkom, J.H., van de Weygaert, R., van der Hulst, J.M., Kovač, K., Yip, C.W., Peebles, P.J.E. (2011), *AJ*, 141, 4

- Kreckel, K., Platen, E., Aragón-Calvo, M.A., van Gorkom, J.H., van de Weygaert, R., van der Hulst, J.M., Beygu, B. (2012), *AJ*, 144, 16
- Kregel, M., van der Kruit, P.C., Freeman, K.C. (2005), *MNRAS*, 358, 503–520
- Kuzio de Naray, R., McGaugh, S.S., de Blok, W.J.G., Bosma, A. (2006), *ApJS*, 165, 461–479
- Kuzio de Naray, R., McGaugh, S.S., de Blok, W.J.G. (2008), *ApJ*, 676, 920–943
- Kwee, K.K., Muller, C.A., Westerhout, G. (1954), *BAN*, 12, 211
- Laine J, Laurikainen E, Salo H, et al. (2014), *MNRAS*, 441, 1992–2012
- Lelli, F., Fraternali, F., Sancisi, R. (2010), *A&A*, 516, A11
- Lelli, F., Verheijen, M., Fraternali, F. (2014) *A&A*, 566, A71
- Lelli, F., McGaugh, S.S., Schombert, J.M. (2016), ArXiv e-prints 1606.09251
- Lewis, B.M. (1968), *Proceedings of the Astronomical Society of Australia*, 1, 104
- Lindblad, P.A.B., Lindblad, P.O., Athanassoula, E. (1996), *A&A*, 313, 65–90
- Lucero, D.M., Carignan, C., Elson, E.C., Randriamampandry, T.H., Jarrett, T.H., Oosterloo, T.A., Heald, G.H. (2015), *MNRAS*, 450, 3935–3951
- Ludlow, A.D., Benitez-Llambay, A., Schaller, M., Theuns, T., Frenk, C.S., Bower, R., Schaye, J., Crain, R.A., Navarro, J.F., Fattahi, A., Oman, K.A. (2016), ArXiv e-prints 1610.07663
- Malin, D., Hadley, B. (1997), *PASA*, 14, 52–58
- Maloney, P. (1993), *ApJ*, 414, 41–56
- Martín-Navarro, I., Bakos, J., Trujillo, I., et al. (2012), *MNRAS*, 427, 1102–1134
- Martínez-Delgado, D., Peñarrubia, J., Gabany, R.J., Trujillo, I., Majewski, S.R., Pohlen, M. (2008), *ApJ*, 689, 184–193
- Martínez-Delgado, D., Gabany, R.J., Crawford, K., et al. (2010), *AJ*, 140, 962–967
- Martínez-Delgado D, Romanowsky AJ, Gabany RJ, et al. (2012), *ApJL*, 748, L24
- Martinsson, T.P.K., Verheijen, M.A.W., Westfall, K.B., Bershad, M.A., Andersen, D.R., Swaters, R.A. (2013), *A&A*, 557, A131
- Martinsson, T.P.K., Verheijen, M.A.W., Bershad, M.A., Westfall, K.B., Andersen, D.R., Swaters, R.A. (2016), *A&A*, 585, A99
- Materne, J., Tammann, G.A. (1976), On the stability of groups of galaxies and the question of hidden matter. In: Kharadze, E.K. (ed.) *Stars and Galaxies from Observational Points of View*, 455–462
- Matthews, L.D., Uson, J.M. (2008), *AJ*, 135, 291–318
- Matthews, L.D., Wood, K. (2003), *ApJ*, 593, 721–732
- McGaugh, S., Lelli, F., Schombert, J. (2016), ArXiv e-prints 1609.05917
- McGee, R.X., Milton, J.A. (1966), *Australian Journal of Physics*, 19, 343
- Meurer, G.R., Carignan, C., Beaulieu, S.F., Freeman, K.C. (1996), *AJ*, 111, 1551
- Milgrom, M. (1983), *ApJ*, 270, 365–370
- Minchin R, Davies J, Disney M, et al. (2007), *ApJ*, 670, 1056–1064
- Mogotsi, K.M., de Blok, W.J.G., Caldú-Primo, A., Walter, F., Ianjamasimanana, R., Leroy, A.K. (2016), *AJ*, 151, 15
- Moore, B. (1994), *Nature*, 370, 629–631
- Mouhcine, M., Ibata, R., Rejkuba, M. (2010), *ApJL*, 714, L12–L15
- Muñoz-Mateos, J.C., Sheth, K., Gil de Paz, A., et al. (2013), *ApJ*, 771, 59
- Muñoz-Mateos, J.C., Sheth, K., Regan, M., et al. (2015), *ApJS*, 219, 3
- Muller, C.A., Oort, J.H. (1951), *Nature*, 168, 357–358
- Navarro, J.F. (1998), ArXiv Astrophysics e-prints astro-ph/9807084
- Navarro, J.F., Frenk, C.S., White, S.D.M. (1996), *ApJ*, 462, 563
- Navarro, J.F., Frenk, C.S., White, S.D.M. (1997), *ApJ*, 490, 493–508
- Newton, K. (1980), *MNRAS*, 191, 169–184
- Newton, K., Emerson, D.T. (1977), *MNRAS*, 181, 573–590
- Noordermeer, E., van der Hulst, J.M., Sancisi, R., Swaters, R.A., van Albada, T.S. (2005), *A&A*, 442, 137–157
- O’Brien, J.C., Freeman, K.C., van der Kruit, P.C. (2010a), *A&A*, 515, A62
- O’Brien, J.C., Freeman, K.C., van der Kruit, P.C. (2010b), *A&A*, 515, A61
- O’Brien, J.C., Freeman, K.C., van der Kruit, P.C. (2010c), *A&A*, 515, A63

- O'Brien, J.C., Freeman, K.C., van der Kruit, P.C., Bosma, A. (2010d), *A&A*, 515, A60
- Oh, S.-H., de Blok, W.J.G., Walter, F., Brinks, E., Kennicutt, R.C. Jr. (2008), *AJ*, 136, 2761–2781
- Oh, S.-H., Brook, C., Governato, F., Brinks, E., Mayer, L., de Blok, W.J.G., Brooks, A., Walter, F. (2011), *AJ*, 142, 24
- Oh, S.-H., Hunter, D.A., Brinks, E., et al. (2015), *AJ*, 149, 180
- Olling, R.P. (1996a), *AJ*, 112, 457
- Olling, R.P. (1996b), The Highly Flattened Dark Matter Halo of NGC 4244. *AJ*, 112, 481
- Olling, R.P., Merrifield, M.R. (2000) *MNRAS*, 311, 361–369
- Oman, K.A., Navarro, J.F., Fattahi, A., et al. (2015), *MNRAS*, 452, 3650–3665
- Oman, K.A., Navarro, J.F., Sales, L.V., Fattahi, A., Frenk, C.S., Sawala, T., Schaller, M., White, S.D.M. (2016), *MNRAS*, 460, 3610–3623
- Oosterloo, T., van Gorkom, J. (2005), *A&A*, 437, L19–L22
- Oosterloo, T., Fraternali, F., Sancisi, R. (2007), *AJ*, 134, 1019
- Ostriker, J.P., Peebles, P.J.E. (1973), *ApJ*, 186, 467–480
- Ostriker, J.P., Peebles, P.J.E., Yahil, A. (1974), *ApJL*, 193, L1–L4
- Ott, J., Walter, F., Brinks, E., Van Dyk, S.D., Dirsch, B., Klein, U. (2001), *AJ*, 122, 3070–3091
- Ott, J., Stilp, A.M., Warren, S.R., Skillman, E.D., Dalcanton, J.J., Walter, F., de Blok, W.J.G., Koribalski, B., West, A.A. (2012), *AJ*, 144, 123
- Peters, S.P.C., van der Kruit, P.C., Allen, R.J., Freeman, K.C. (2013), *ArXiv e-prints*, 1303.2463
- Peters, S.P.C., de Geyter, G., van der Kruit, P.C., Freeman, K.C. (2016a), *ArXiv e-prints* 1608.05563
- Peters, S.P.C., van der Kruit, P.C., Allen, R.J., Freeman, K.C. (2016b), *ArXiv e-prints* 1608.05557
- Peters, S.P.C., van der Kruit, P.C., Allen, R.J., Freeman, K.C. (2016c), *ArXiv e-prints* 1608.05559
- Peters, S.P.C., van der Kruit, P.C., Allen, R.J., Freeman, K.C. (2016d), *ArXiv e-prints* 1605.08209
- Ponomareva, A.A., Verheijen, M.A.W., Bosma, A. (2016), *MNRAS*, 463, 4052–4067
- Puche, D., Westpfahl, D., Brinks, E., Roy, J.R. (1992), *AJ*, 103, 1841–1858
- Radburn-Smith, D.J., de Jong, R.S., Streich, D., et al. (2014), *ApJ*, 780, 105
- Rand, R.J., Kulkarni, S.R., Hester, J.J. (1990), *ApJL*, 352, L1–L4
- Randriamampandry, T.H., Carignan, C. (2014), *MNRAS*, 439, 2132–2145
- Read, J.I., Iorio, G., Agertz, O., Fraternali, F. (2016), *MNRAS*, 462, 3628–3645
- Rich, R.M., Collins, M.L.M., Black, C.M., Longstaff, F.A., Koch, A., Benson, A., Reitzel, D.B. (2012), *Nature*, 482, 192–194
- Roberts, M.S. (1966), *ApJ*, 144, 639
- Roberts, M.S. (1972), In: Evans, D.S., Wills, D., Wills, B.J. (eds.) *External Galaxies and Quasi-Stellar Objects*, IAU Symposium, vol 44, p 12
- Roberts, M.S. (1975), In: Hayli, A. (ed.) *Dynamics of Stellar Systems*, IAU Symposium, vol 69, p 331
- Roberts, M.S. (1988), How Much of the Universe Do We See? In: *Bicentennial commemoration of R.G. Boscovich* : Milano, September 15-18, Bossi, M, Tucci, P. (eds.), 237-247.
- Roberts, M.S., Rots, A.H. (1973), *A&A*, 26, 483–485
- Roberts, M.S., Whitehurst, R.N. (1975), *ApJ*, 201, 327–346
- Rogstad, D.H. (1971), Aperture synthesis study of neutral hydrogen in the galaxy M101: II. Discussion. *A&A*, 13, 108–115
- Rogstad, D.H., Shostak, G.S. (1971), *A&A*, 13, 99–107
- Rogstad, D.H., Shostak, G.S. (1972) *ApJ*, 176, 315
- Rogstad, D.H., Lockhart, I.A., Wright, M.C.H. (1974), *ApJ*, 193, 309–319
- Rogstad, D.H., Wright, M.C.H., Lockhart, I.A. (1976), *ApJ*, 204, 703–711
- Rogstad, D.H., Chu, K., Crutcher, R.M. (1979), *ApJ*, 229, 509–513
- Roychowdhury, S., Chengalur, J.N., Begum, A., Karachentsev, I.D. (2010), *MNRAS* 404:L60–L63,

- Roychowdhury, S., Chengalur, J.N., Karachentsev, I.D., Kaisina, E.I. (2013), *MNRAS*, 436, L104–L108
- Rubin, V.C., Ford, W.K. Jr. (1970), *ApJ*, 159, 379
- Rubin, V.C., Thonnard, N., Ford, W.K. Jr. (1978), *ApJL*, 225, L107–L111
- Rubin, V.C., Ford, W.K. Jr., Thonnard, N. (1980), *ApJ*, 238, 471–487
- Rubin, V.C., Ford, W.K. Jr., Thonnard, N., Burstein, D. (1982), *ApJ*, 261, 439–456
- Rubin, V.C., Burstein, D., Ford, W.K. Jr., Thonnard, N. (1985), *ApJ*, 289, 81–98
- Rupen, M.P. (1991), *AJ*, 102, 48–106
- Sackett, P.D., Morrison, H.L., Harding, P., Boroson, T.A. (1994a), *Nature*, 370, 441–443
- Sackett, P.D., Rix, H.-W., Jarvis, B.J., Freeman, K.C. (1994b), *ApJ*, 436, 629–641
- Saha, K., de Jong, R., Holwerda, B. (2009), *MNRAS*, 396, 409–422
- Salpeter, E.E. (1978), In: Berkhuijsen, E.M., Wielebinski, R. (eds.) *Structure and Properties of Nearby Galaxies*, IAU Symposium, vol 77, pp 23–26
- Sancisi, R. (1976), *A&A*, 53, 159
- Sancisi, R., Allen, R.J. (1979), *A&A*, 74, 73–84
- Sancisi, R., Fraternali, F., Oosterloo, T., van der Hulst, T. (2008), *A&AR*, 15, 189–223
- Sandage, A. (1961), *The Hubble atlas of galaxies*, Washington: Carnegie Institution
- Sandage, A., Freeman, K.C., Stokes, N.R. (1970), *ApJ*, 160, 831
- Sanders, R.H., McGaugh, S.S. (2002), *ARAA*, 40, 263–317,
- Schmidt, M. (1957), *BAN*, 14, 17
- Schwarzschild, M. (1954), *AJ*, 59, 273
- Schweizer, F., Whitmore, B.C., Rubin, V.C. (1983), *AJ*, 88, 909–925
- Serra P, Oosterloo T, Morganti R, et al. (2012), *MNRAS*, 422, 1835–1862
- Serra P, Oser L, Krajinović D, et al. (2014), *MNRAS*, 444, 3388–3407
- Shobbrook, R.R., Robinson, B.J. (1967), *Australian Journal of Physics*, 20, 131
- Shostak, G.S., van der Kruit, P.C. (1984), *A&A*, 132, 20–32
- Simon, J.D., Bolatto, A.D., Leroy, A., Blitz, L. (2003), *ApJ*, 596, 957–981
- Simon, J.D., Bolatto, A.D., Leroy, A., Blitz, L., Gates, E.L. (2005), *ApJ*, 621, 757–776
- Stanonik, K., Platen, E., Aragón-Calvo, M.A., van Gorkom, J.H., van de Weygaert, R., van der Hulst, J.M., Peebles, P.J.E. (2009), *ApJL*, 696, L6–L9
- Stilp, A.M., Dalcanton, J.J., Skillman, E., Warren, S.R., Ott, J., Koribalski, B. (2013a), *ApJ*, 773, 88
- Stilp, A.M., Dalcanton, J.J., Warren, S.R., Skillman, E., Ott, J., Koribalski, B. (2013b), *ApJ*, 765, 136
- Streich, D., de Jong, R.S., Bailin, J., Bell, E.F., Holwerda, B.W., Minchev, I., Monachesi, A., Radburn-Smith, D.J. (2016), *A&A*, 585, A97
- Sunyaev, R.A. (1969), *ApL*, 3, 33
- Swaters, R.A., Sancisi, R., van der Hulst, J.M. (1997), *ApJ*, 491, 140–145
- Swaters, R.A., van Albada, T.S., van der Hulst, J.M., Sancisi, R. (2002), *A&A*, 390, 829–861
- Swaters, R.A., Madore, B.F., van den Bosch, F.C., Balcells, M. (2003), *ApJ*, 583, 732–751
- Tamburro, D., Rix, H.-W., Leroy, A.K., Mac Low, M.M., Walter, F., Kennicutt, R.C., Brinks, E., de Blok, W.J.G. (2009), *AJ*, 137, 4424–4435
- Thilker, D.A., Bianchi, L., Meurer, G., et al. (2007), *ApJS*, 173, 538–571
- Tollet, E., Macciò, A.V., Dutton, A.A., et al. (2016), *MNRAS*, 456, 3542–3552
- Toloba, E., Guhathakurta, P., Romanowsky, A.J., Brodie, J.P., Martínez-Delgado, D., Arnold, J.A., Ramachandran, N., Theakanath, K. (2016), *ApJ*, 824, 35
- Toomre, A. (1981), In: Fall, S.M., Lynden-Bell, D. (eds.) *Structure and Evolution of Normal Galaxies*, pp 111–136
- Trott, C.M., Treu, T., Koopmans, L.V.E., Webster, R.L. (2010), *MNRAS*, 401, 1540–1551
- Uson, J.M., Matthews, L.D. (2003), *AJ*, 125, 2455–2472
- Van Albada, T.S., Sancisi, R. (1986), *Philosophical Transactions of the Royal Society of London Series A*, 320, 447–464
- van de Hulst, H.C., Raimond, E., van Woerden, H. (1957), *BAN*, 14, 1
- van der Hulst, T., Sancisi, R. (1988), *AJ*, 95, 1354–1359

- van der Kruit, P.C. (1979), *A&AS*, 38, 15–38
- van der Kruit, P.C. (1981), *A&A*, 99, 298–304
- van der Kruit, P.C. (2007), *A&A*, 466, 883–893
- van der Kruit, P.C., Shostak, G.S. (1982), *A&A*, 105, 351–358
- van der Kruit, P.C., Shostak, G.S. (1984), *A&A*, 134, 258–267
- van Woerden, H., Bosma, A., Mebold, U. (1975), In: Weliachew, L. (ed.) *La Dynamique des galaxies spirales*, vol 241, 483
- van Zee, L. (2004), *Bulletin of the American Astronomical Society*, vol 36, 1495
- Verdes-Montenegro, L., Yun, M.S., Williams, B.A., Huchtmeier, W.K., Del Olmo, A., Perea, J. (2001), *A&A*, 377, 812–826
- Verdes-Montenegro, L., Bosma, A., Athanassoula, E. (2002), *A&A*, 389, 825–835
- Verheijen, M.A.W., Sancisi, R. (2001), *A&A*, 370, 765–867
- Volders, L.M.J.S. (1959), *BAN*, 14, 323
- Walter, F., Brinks, E., de Blok, W.J.G., Bigiel, F., Kennicutt, R.C. Jr., Thornley, M.D., Leroy, A. (2008), *AJ*, 136, 2563–2647
- Wang, J., Kauffmann, G., Józsa, G.I.G., et al. (2013), *MNRAS*, 433, 270–294
- Wang, J., Koribalski, B.S., Serra, P., van der Hulst, T., Roychowdhury, S., Kamphuis, P., Chengalur, J.N. (2016), *MNRAS*, 460, 2143–2151
- Weiner, B.J. (2004), In: Ryder, S., Pisano, D., Walker, M., Freeman, K. (eds.) *Dark Matter in Galaxies*, IAU Symposium, vol 220, 265
- Weiner, B.J., Sellwood, J.A., Williams, T.B. (2001), *ApJ*, 546, 931–951
- Westfall, K.B., Bershad, M.A., Verheijen, M.A.W. (2011), *ApJS*, 193, 21
- Westmeier, T., Braun, R., Koribalski, B.S. (2011), *MNRAS*, 410, 2217–2236
- Westmeier, T., Koribalski, B.S., Braun, R. (2013), *MNRAS*, 434, 3511–3525
- White, S.D.M., Rees, M.J. (1978), *MNRAS*, 183, 341–358
- Whitmore, B.C., McElroy, D.B., Schweizer, F. (1987), *ApJ*, 314, 439–456
- Wilkinson, P.N. (1991), In: Cornwell, T.J., Perley, R.A. (eds.) *IAU Colloq. 131: Radio Interferometry. Theory, Techniques, and Applications*, ASP Conference Series, vol 19, 428–432
- Wolfe, S.A., Pisano, D.J., Lockman, F.J., McGaugh, S.S., Shaya, E.J. (2013), *Nature*, 497, 224–226
- Wolfinger, K., Kilborn, V.A., Ryan-Weber, E.V., Koribalski, B.S. (2016), *PASA*, 33, e038
- Zánmar Sánchez, R., Sellwood, J.A., Weiner, B.J., Williams, T.B. (2008), *ApJ*, 674, 797–813
- Zheng, Z., Shang, Z., Su, H., et al. (1999), *AJ*, 117, 2757–2780